

# How Large Are the Bars in Barred Galaxies?

Peter Erwin<sup>1,2,3\*</sup>

<sup>1</sup>*Instituto de Astrofísica de Canarias, C/ Vía Láctea s/n, 38200 La Laguna, Tenerife, Spain*

<sup>2</sup>*Current address: Max-Planck-Institut für extraterrestrische Physik, Giessenbachstrasse, D-85748 Garching, Germany*

<sup>3</sup>*Guest investigator of the UK Astronomy Data Centre*

1 November 2018

## ABSTRACT

I present a study of the sizes (semimajor axes) of bars in disc galaxies, combining a detailed  $R$ -band study of 65 S0–Sb galaxies with the  $B$ -band measurements of 70 Sb–Sd galaxies from Martin (1995). As has been noted before with smaller samples, bars in early-type (S0–Sb) galaxies are clearly larger than bars in late-type (Sc–Sd) galaxies; this is true both for relative sizes (bar length as fraction of isophotal radius  $R_{25}$  or exponential disc scale length  $h$ ) and absolute sizes (kpc). S0–Sb bars extend to  $\sim 1$ – $10$  kpc (mean  $\sim 3.3$  kpc),  $\sim 0.2$ – $0.8$   $R_{25}$  (mean  $\sim 0.38$   $R_{25}$ ) and  $\sim 0.5$ – $2.5$   $h$  (mean  $\sim 1.4$   $h$ ). Late-type bars extend to only  $\sim 0.5$ – $3.5$  kpc,  $\sim 0.05$ – $0.35$   $R_{25}$  and  $0.2$ – $1.5$   $h$ ; their mean sizes are  $\sim 1.5$  kpc,  $\sim 0.14$   $R_{25}$  and  $\sim 0.6$   $h$ . Sb galaxies resemble earlier-type galaxies in terms of bar size relative to  $h$ ; their smaller  $R_{25}$ -relative sizes may be a side effect of higher star formation, which increases  $R_{25}$  but not  $h$ . Sbc galaxies form a transition between the early- and late-type regimes. For S0–Sbc galaxies, bar size correlates well with disc size (both  $R_{25}$  and  $h$ ); these correlations are stronger than the known correlation with  $M_B$ . All correlations appear to be weaker or absent for late-type galaxies; in particular, there seems to be *no* correlation between bar size and either  $h$  or  $M_B$  for Sc–Sd galaxies.

Since bar size scales with disc size and galaxy magnitude for most Hubble types, studies of bar evolution with redshift should select samples with similar distributions of disc size or magnitude (extrapolated to present-day values); otherwise, bar frequencies and sizes could be mis-estimated. Because early-type galaxies tend to have larger bars, resolution-limited studies will preferentially find bars in early-type galaxies (assuming no significant differential evolution in bar sizes). I show that the bars detected in *HST* near-IR images at  $z \sim 1$  by Sheth et al. (2003) have absolute sizes consistent with those in bright, nearby S0–Sb galaxies. I also compare the sizes of real bars with those produced in simulations, and discuss some possible implications for scenarios of secular evolution along the Hubble sequence. Simulations often produce bars as large as – or larger than – those seen in S0–Sb galaxies, but rarely any as small as those in Sc–Sd galaxies.

**Key words:** galaxies: structure – galaxies: elliptical and lenticular, cD – galaxies: spiral – galaxies: evolution.

## 1 INTRODUCTION

Observations indicate that  $\sim 70\%$  of all disc galaxies are barred to one degree or another (e.g., Eskridge et al. 2000; Erwin 2005). There is considerable debate about the origin and influence of bars, and also about their strengths, something for which there is still no agreed-upon measurement, though many have been suggested (e.g., Martin 1995; Seigar & James 1998; Chapelon et al. 1999; Buta & Block 2001). Curiously, somewhat less attention has been given to

the question of bar *sizes*, perhaps because this seems, on the face of it, easier to measure – even though there are no agreed-upon methods of measuring bar sizes either (see the discussions in Athanassoula & Misiriotis 2002 and Aguerri et al. 2003).

Is bar size actually important? There are, I would argue, several reasons why bar size is interesting, beyond a basic natural historian’s curiosity (“Just how big or small *are* they, anyway?”). To begin with, the size of a bar is first approximation to how much of its host galaxy can be affected by the bars’ dynamical influence: larger bars can obviously affect more of the galaxy than smaller bars. In addition to

\* E-mail: erwin@mpe.mpg.de

the well-known effects of bars on gas flow, Weinberg & Katz (2002) and Holley-Bockelmann et al. (2005) argued that bars can also restructure dark-matter halos, flattening out the steep central cusps which are produced in cosmological simulations but apparently not seen in real galaxies (but see Sellwood 2003; Athanassoula 2004). Larger bars could then mean larger dark-matter cores. Holley-Bockelmann et al. also argued that tidally-induced bars could be significantly larger than the “classical”  $n$ -body bars which form via disc instabilities, so bar size may provide clues to past merger histories. More generally, bar size is an obvious way of testing the accuracy of different bar-formation and bar-evolution models (e.g., Valenzuela & Klypin 2003). For example, Bournaud & Combes (2002) recently outlined a scenario of galaxy evolution involving multiple rounds of bar formation, self-destruction, and resurrection due to gas accretion; they predict a trend of bar size with Hubble type, where galaxies with larger bulges (i.e., earlier Hubble types) have shorter bars.  $N$ -body simulations also suggest that bar size depends on angular momentum exchange between the bar and the bulge, the outer disc, and the halo. Since the relative masses of these components, as well as how kinematically hot they are, can affect how much angular momentum is exchanged (e.g., Athanassoula 2003), bar size could be a useful probe of halo mass and kinematics. Finally, several studies have suggested that longer bars are correlated with higher star formation activity, at least in late-type galaxies (e.g., Martinet & Friedli 1997; Chapelon et al. 1999).

The first systematic investigation of bar sizes was made by Kormendy (1979), who found that bar size correlated with galaxy blue luminosity. Subsequently, Elmegreen & Elmegreen (1985, hereafter EE85) showed that bars in early-type disc galaxies tended to be larger, relative to the optical disc diameter  $D_{25}$ , than bars in later Hubble types (see also Regan & Elmegreen 1997). They also found a dichotomy in bar *structure*: early-type galaxies typically have bars with shallow (“flat”) profiles and truncations (as noted by Kormendy 1982), while late-type galaxies tend to have bars with steep exponential profiles. More recent studies using CCDs or near-infrared images include those of Chapelon et al. (1999), Laine et al. (2002), and Laurikainen and collaborators (Laurikainen & Salo 2002; Laurikainen et al. 2002); these have, in general, supported the findings of Kormendy and EE85.

Because a number of these studies have focused on particular subtypes of galaxies, the results are not as general or unbiased as they might otherwise be. For example, Chapelon et al. (1999) studied primarily a large sample of starburst galaxies, while the studies of Laine et al. (2002) and Laurikainen et al. (2002) were aimed at Seyfert and other “active” galaxies. Chapelon et al. noted that bar sizes for their late-type (starburst) galaxies tended to be larger than those of the normal late-type galaxies of Martin (1995); similarly, Laurikainen et al. found that Seyferts tended to have larger bars than non-Seyferts. Except for the pioneering studies of Kormendy and EE85, bars in the earliest disc galaxies – i.e., S0 galaxies – have been ignored or represented by only a handful of examples. Finally, there has also been a tendency to overlook so-called “weak” (i.e., SAB) bars: the samples of Kormendy and EE85 are almost entirely SB galaxies, and bar sizes were measured by Laurikainen et al.

only for galaxies with relatively high  $m = 2$  Fourier bar amplitudes.

Thus, there is still considerable room for improving our understanding of bar sizes in the general population of disc galaxies, especially for S0 galaxies and weak bars. The relevance of bar size distributions for galaxy evolution was recently highlighted by Sheth et al. (2003), who discussed the visibility of bars as a function of redshift and resolution. Put simply, large bars (size in kpc) are easier to detect at high redshift than small bars; if the average bar is small enough, it will be undetectable at high  $z$ . Failure to account for this possibility can produce spurious changes in bar fraction with redshift. (We might also like to know if the average bar size has changed significantly between, say,  $z = 1$  and now, which presupposes a good understanding of local bar sizes.)

In this paper, I take a detailed look at the question of bar sizes along the Hubble sequence in the local universe. The main part of this study uses a diameter-limited sample of nearby, early-type (S0–Sb) disc galaxies with both strong (SB) and weak (SAB) bars. I measure the bar lengths and compare them with the overall size of the galaxy, using both the 25th-magnitude radius ( $R_{25}$ ) and the exponential scale lengths of the outer discs. These are combined with the measurements of Martin (1995), which also include both SB and SAB bars and are primarily of later Hubble types (Sbc–Sd).

## 2 SAMPLES

I use two samples of galaxies in this paper. The first is a sample of early-type (S0–Sb) galaxies, using recent  $R$ -band imaging for both bar-size and exponential disc scale length measurements; both sets of measurements are presented here. To extend this study to later Hubble types, I have drawn on a second sample, that of Martin (1995). This consists primarily of Sb–Sd galaxies, with bar-size measurements made from blue photographic prints.

The early-type galaxy sample is an expanded version of that presented in Erwin & Sparke (2003); I will refer to their original sample as the “WIYN Sample” (since most of the observations were made with the 3.5m WIYN Telescope).<sup>1</sup> The WIYN Sample consists of all optically barred (SB + SAB) S0–Sa galaxies from the UGC catalog (Nilson 1973) which met the following criteria: declination  $> 10^\circ$ , heliocentric radial velocity  $\leq 2000 \text{ km s}^{-1}$ , major axis diameter  $\geq 2'$ , and ratio of major to minor axis  $a/b \leq 2$  (corresponding to  $i \lesssim 60^\circ$ ). Galaxy types and axis measurements (at the 25 mag arcsec<sup>−2</sup> level in  $B$ ) were taken from de Vaucouleurs et al. (1991, hereafter RC3); radial velocities are from the NASA/IPAC Extragalactic Database (NED). The size restriction and the use of the UGC means that the sample is biased in favor of bright, high surface brightness galaxies. The sample had a total of 38 galaxies; I subsequently eliminated four galaxies where bars were either absent, ambiguous, or too difficult to measure (see the Appendix), leaving a total of 34 S0–Sa galaxies.

There is some evidence that Hubble types in clusters

<sup>1</sup> The WIYN Observatory is a joint facility of the University of Wisconsin-Madison, Indiana University, Yale University, and the National Optical Astronomy Observatories

– in the Virgo Cluster, at least – do not agree with Hubble types of isolated field galaxies (van den Bergh 1976). Koopman & Kenney (1998) found that Virgo Sa–Sab galaxies had central light concentrations more like those of isolated Sb–Sc field galaxies. Accordingly, Erwin & Sparke excluded Virgo galaxies from their sample. Because the case for S0 galaxies is unclear (Koopman & Kenney noted that their sample was strongly incomplete for S0 galaxies, and the few S0 galaxies they studied did not differ significantly between field and Virgo – see their Figure 1), and because information on bar sizes in S0 galaxies is particularly lacking, I have added bar measurements for eight of the ten barred S0’s in Virgo which meet the criteria given above, except for the redshift limit. (The redshift limit was intended to set a distance limit of  $\sim 30$  Mpc for the field galaxies; if it were applied to the Virgo Cluster, which lies well within that distance, it would improperly exclude cluster galaxies with high peculiar velocities.)

To make the coverage of Hubble types more complete, I have also added galaxies from an ongoing study of barred Sab and Sb galaxies (Erwin, Vega Beltrán & Beckman, in preparation). The selection criteria are identical, aside from the difference in Hubble type, leading to a total of 9 Sab and 18 Sb galaxies; two of each type appear to be unbarred, and are not considered further (see the Appendix).

The final early-type sample thus has a total of 65 strongly and weakly barred S0–Sb galaxies. All of these galaxies, grouped by Hubble type, are listed in Table 1, along with the parameters of their bars and outer discs.

The sample which best complements mine is that of Martin (1995): it is large and drawn from ordinary, optically barred galaxies (including both SB and SAB classes), contains both observed and deprojected bar lengths, and is almost entirely Sb or later in Hubble type. To make the match between samples as close as possible, I applied the same selection criteria to Martin’s galaxies: SB or SAB bar classification, major axis  $\geq 2'$ , axis ratio  $\leq 2$ , and radial velocity  $\leq 2000 \text{ km s}^{-1}$ . Martin argued that deprojection was unreliable for Magellanic galaxies (Sm and Im), so I follow him in excluding those types. I also removed three Virgo galaxies (NGC 4303, NGC 4321, and NGC 4394) and eliminated NGC 4395, which is classed as SA in RC3; for the three galaxies in common between the samples (see below), I retain my measurements. This leaves a total of 75 galaxies from his sample, still large enough for a good comparison; the bulk of these (70) are Sb–Sd. To these I added distances and total blue magnitudes, mostly from LEDA (see Appendix A4 for details). Although the underlying sample selection was different (Martin’s galaxies were taken from the Sandage-Bedke atlas), the relative numbers of different Hubble types are consistent with local populations. For example, my sample has 24 S0/a–Sab galaxies compared with 56 Sbc–Scd galaxies in Martin’s sample; the ratio of late to early types (2.3) is similar to that found in RC3 for galaxies with  $D_{25} \geq 2.0'$  and  $a/b \leq 2.0$  (480 Sbc–Scd galaxies versus 199 S0/a–Sab, for a ratio of 2.4). This suggests that the combined set provides a reasonable picture of bar sizes for the Hubble sequence down to Sd (Martin’s sample has very few Sdm or Sm galaxies), at least for bright galaxies (median  $M_B = -19.5$  for my S0–Sb galaxies and  $-19.8$  for Martin’s Sb–Sd; see Figure 1).

For the early-type galaxies, the measurements of bar

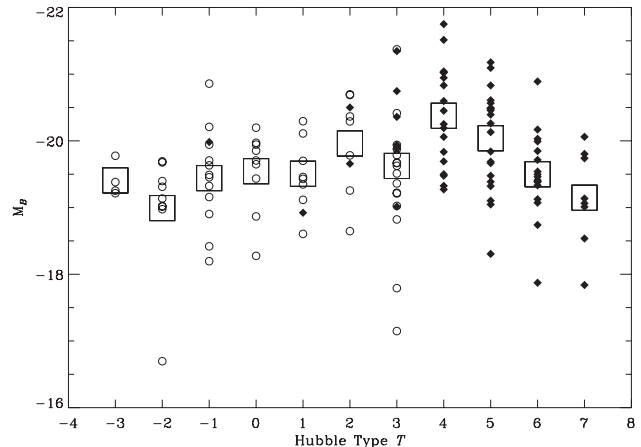


**Figure 1.** Absolute blue magnitudes for galaxies from the two samples as a function of Hubble type. Galaxies from my sample are shown with open circles, while galaxies from Martin (1995) meeting the same selection criteria are shown with filled diamonds; mean values for each Hubble type are indicated by the large boxes.

size and shape, and of disc sizes, are discussed in Sections 3.1–3.3, below. In Section 3.4, I discuss how the published bar sizes of Martin (1995) can best be compared with my measurements, and how I obtained disc scale lengths for Martin’s galaxies.

### 3 OBSERVATIONS AND MEASUREMENTS

Observations of the original WIYN Sample (S0–Sa galaxies) are presented and discussed in detail by Erwin & Sparke (2003). All but two of the galaxies were observed in *B* and *R* with the 3.5 m WIYN Telescope at Kitt Peak, Arizona, between 1995 December and 1998 March. Images for NGC 936 and NGC 4314 were taken from the BARS Project observations (Lourenço & Beckman 2001); in a few cases, additional images from other sources were used for outer-disc or bar measurements (see the Appendix for details).

Images of the barred Virgo S0 galaxies and the Sab–Sb galaxies are from a variety of sources, including the WIYN Telescope (1995 March through 1998 March); the 2.4 m MDM Telescope at Kitt Peak, courtesy Paul Schechter (1996 March); the 2.5 m Nordic Optical Telescope in La Palma (2001 April and 2002 April); and the Isaac Newton Group archive (images from both the 1 m Jacobus Kapteyn Telescope and the 2.5 m Isaac Newton Telescope). The outer-disc scale lengths for several galaxies were measured using images taken with the Isaac Newton Telescope in 2004 March; these observations will be described in more detail in Erwin, Pohlen, & Beckman (in preparation). I also used observations from the BARS Project (for NGC 4151 and NGC 4596) and *r*- or *R*-band images from the sample of Frei et al. (1996) for a number of galaxies. Specific details for individual galaxies are discussed in the Appendix.

Except where noted in the Appendix (cases where dust severely distorted bar isophotes in the optical images), all bar and outer-disc scale length measurements were made with *R*-band or equivalent images. For Sab and Sb galaxies, these measurements were usually checked against mea-

measurements made with near-IR images; the agreement was generally very good.

Parameters for these galaxies are listed in Table 1. Most distances are from LEDA (exceptions are discussed in the Appendix); the latter are based on redshifts corrected for Virgocentric infall, as listed in LEDA, and assuming  $H_0 = 75 \text{ km s}^{-1} \text{ kpc}^{-1}$ . For Virgo galaxies, I assumed a default distance to the Virgo Cluster of 15.3 Mpc (Freedman et al. 2001), except for NGC 4754, for which a surface-brightness fluctuation measurement by Tonry et al. (2001) is available. Note that distance measurements, and their uncertainties, only affect the *absolute* sizes of bars; relative bar sizes are distance-independent.

### 3.1 Measuring the Sizes of Bars

There is no standard way to measure the length of a bar, either for real galaxies or for simulations. Methods which have been used for real galaxies include: visual estimation directly from images (e.g., Kormendy 1979; Martin 1995); fitting ellipses to the galaxy isophotes, with bar length usually determined from a maximum in the ellipticity (e.g., Wozniak & Pierce 1991; Wozniak et al. 1995; Jungwiert et al. 1997; Laine et al. 2002; Sheth et al. 2003); various measurements based on Fourier analysis of the galaxy image, using either the bar-interbar luminosity contrast (e.g., Ohta et al. 1990; Aguerri et al. 2000) or the phase angle (e.g., Quillen et al. 1994); and measurements using the major-axis profile of the bar (e.g., Seigar & James 1998; Chapelon et al. 1999). There is similar variation in how bars are measured even when the galaxy is readily accessible; i.e., in  $n$ -body simulations – compare, for example, Debattista & Sellwood (2000), Athanassoula & Misiriotis (2002), and Valenzuela & Klypin (2003). As Athanassoula & Misiriotis demonstrate, different methods applied to the same (model) galaxies can lead to variations of  $\sim 15$ –35% in measured length.<sup>2</sup>

After some experimentation, I settled on two measurements, an approach I also used for the outer and inner bars of double-barred galaxies (Erwin 2004). These can be thought of as lower and upper limits on the bar size. The lower-limit measurement is  $a_e$ , the semimajor axis of maximum ellipticity in the bar region, which is useful primarily because it is common and reproducible. In some cases, there is no clear ellipticity peak associated with the bar; but a corresponding extremum in the *position angles* can often be found which serves the same purpose; examples include NGC 2880 and NGC 4143 (see Erwin & Sparke 2003). It is important to stress that I identify  $a_e$  with the maximum in ellipticity (or maximum deviation in position angle) *closest to the end of the bar, but still inside the bar*. In some cases, particularly when there are strong dust lanes and/or star formation, the inner isophotes can become highly distorted and *more* elliptical than the bar proper; examples include NGC 2787, IC 676, and NGC 4691 (Erwin & Sparke 2003).<sup>3</sup> In other cases, the bar merges so smoothly into spiral arms further

out that the “obvious” maximum in ellipticity occurs well outside the bar and is due to spiral arms or a ring. Examples of this include NGC 3185 and NGC 7743 (Erwin & Sparke 2003); another good example, albeit a galaxy not in this study, is NGC 4303 (see the discussion in Erwin 2004).

Despite the relative simplicity and common use of  $a_e$ , there is good reason to believe that it underestimates the true length of the bar. This has been pointed out by several authors (Wozniak et al. 1995; Erwin & Sparke 2003; Laurikainen et al. 2002), and Athanassoula & Misiriotis (2002) found that it generally provided the smallest estimates of bar length in their  $n$ -body simulations. Thus there is a need for a second (“upper-limit”) measurement, which I refer to as the bar’s “length”  $L_{\text{bar}}$ . This is based on the approach of Erwin & Sparke (2003), where the bar length was defined as the *minimum* of two ellipse-fit measures: the first minimum in ellipticity outside the bar’s peak ellipticity ( $a_{\text{min}}$ ), or the point at which the position angles of the fitted ellipses differ by  $\geq 10^\circ$  from the bar’s position angle. To their definition, I have added a qualification: if the bar is surrounded by a ring or spiral arms, and the size of the ring (or arms, where they intersect the bar) is smaller than either  $a_{\text{min}}$  or  $a_{10}$ , then I adopt the ring/spiral size. This is because chance combinations of orientation and projection acting on the ring or spirals can lead to ellipse-fit profiles that place  $a_{\text{min}}$  and  $a_{10}$  well *outside* the bar. Since there is no indication in any of these galaxies that the bar extends beyond the ring or surrounding spirals, it makes sense to use the latter as an upper limit on bar size. Table 1 lists  $a_e$ ,  $a_{\text{min}}$ ,  $a_{10}$ , and the adopted  $L_{\text{bar}}$  for each galaxy; if  $L_{\text{bar}}$  is smaller than either  $a_{\text{min}}$  or  $a_{10}$ , then this means that  $L_{\text{bar}}$  was derived using rings or spiral arms.

The  $L_{\text{bar}}$  measurement is perhaps less consistent and accurate than  $a_e$  (it is prone to strongly overestimate bar length in face-on galaxies lacking rings or spiral arms), but may give a better measure of the bar’s “true” length – that is, where the bar distortion finally gives way to the outer disc or spiral structure. The only galaxy where it clearly fails is NGC 4203, which is face-on and lacking in any spiral arms or rings, so that  $a_{\text{min}} = 46''$  even though  $a_e = 13''$ ; consequently, I exclude that galaxy from statistics using  $L_{\text{bar}}$ .

In practice, the two measurements are extremely well correlated (Figure 2); the Pearson and Spearman correlation coefficients are  $r = 0.96$  and  $r_s = 0.95$ , respectively.<sup>4</sup> The mean (deprojected) ratio of  $a_e/L_{\text{bar}}$  is 0.80. This is not too far from the mean ratio (0.73) of sizes for the  $L_{b/a}$  and  $L_{\text{phase}}$  measurements of Athanassoula & Misiriotis (2002), which suggests that those two  $n$ -body bar measurements are a good match to  $a_e$  and  $L_{\text{bar}}$  (see Section 5.2).

The position angles of the bars are also needed, since I use them to deproject bar sizes. As shown by Erwin & Sparke (2003), ellipse fits are a problematic source for bar position angles. Their Table 5 lists 11 large-scale bars whose position angles differ from those given by the ellipse fits by more than  $5^\circ$ ; see their Figures 5 and 6 for examples. Thus, bar position angles are *always* checked against the im-

<sup>2</sup> Based on the mean and standard deviations from their Table 1.

<sup>3</sup> This can happen even in the near-IR: Laurikainen & Salo (2002) report an unusually small  $a_e = 18''$  for NGC 4691, from ellipse fits to 2MASS images.

<sup>4</sup> As a reminder, the Pearson coefficient measures the strength of *linear* correlations; the Spearman coefficient measures general correlations and is usually considered more robust against outliers; see, e.g., Press et al. (1996).

**Table 1.** Bar and Disc Measurements for S0–Sb Galaxies

| Name              | Type                     | Distance<br>(Mpc) | $M_B$  | Outer Disc         |                     |                      |                 | Bar                |                   |                               |                              |                         |
|-------------------|--------------------------|-------------------|--------|--------------------|---------------------|----------------------|-----------------|--------------------|-------------------|-------------------------------|------------------------------|-------------------------|
|                   |                          |                   |        | PA<br>( $^\circ$ ) | $i$<br>( $^\circ$ ) | $R_{25}$<br>( $''$ ) | $h$<br>( $''$ ) | PA<br>( $^\circ$ ) | $a_e$<br>( $''$ ) | $a_{\min}/a_{10}$<br>( $''$ ) | $L_{\text{bar}}$<br>( $''$ ) | $\epsilon_{\text{max}}$ |
| S0 Galaxies       |                          |                   |        |                    |                     |                      |                 |                    |                   |                               |                              |                         |
| NGC 936           | SB(rs)0 <sup>+</sup>     | 23.0              | −20.86 | 130                | 41                  | 140                  | ...             | 81                 | 41                | 65/ 51                        | 51                           | 0.47                    |
| NGC 2787          | SB(r)0 <sup>+</sup>      | 7.5               | −18.20 | 109                | 55                  | 95                   | 27              | 160                | 29                | 36/ 36                        | 36                           | 0.34                    |
| NGC 2859          | (R)SB(r)0 <sup>+</sup>   | 24.2              | −20.21 | 90                 | 25                  | 128                  | ...             | 162                | 34                | 52/ 43                        | 43                           | 0.40                    |
| NGC 2880          | SB0 <sup>−</sup>         | 21.9              | −19.38 | 144                | 52                  | 62                   | ...             | 82                 | 8                 | 9/ 10                         | 9                            | 0.20                    |
| NGC 2950          | (R)SB(r)0 <sup>0</sup>   | 14.9              | −19.14 | 120                | 48                  | 80                   | 32              | 162                | 24                | 41/ 31                        | 31                           | 0.43                    |
| NGC 2962          | (R)SAB(rs)0 <sup>+</sup> | 30.0              | −19.71 | 7                  | 53                  | 79                   | ...             | 168                | 29                | 43/...                        | 43                           | 0.30                    |
| NGC 3412          | SB(s)0 <sup>0</sup>      | 11.3              | −18.98 | 152                | 58                  | 109                  | ...             | 100                | 15                | 21/ 21                        | 21                           | 0.26                    |
| NGC 3489          | SAB(rs)0 <sup>+</sup>    | 12.1              | −19.45 | 71                 | 58                  | 106                  | 17              | 12                 | 13                | .../ 17                       | 17                           | 0.17                    |
| NGC 3941          | SB(s)0 <sup>0</sup>      | 12.2              | −19.31 | 9                  | 52                  | 104                  | 25              | 166                | 21                | 36/ 32                        | 32                           | 0.47                    |
| NGC 3945          | (R)SB(rs)0 <sup>+</sup>  | 19.8              | −19.94 | 158                | 55                  | 158                  | ...             | 72                 | 32                | 41/ 39                        | 39                           | 0.29                    |
| NGC 4143          | SAB(s)0 <sup>0</sup>     | 15.9              | −19.40 | 144                | 59                  | 68                   | 14              | 163                | 17                | .../ 28                       | 28                           | 0.38                    |
| NGC 4203          | SAB0 <sup>−</sup>        | 15.1              | −19.21 | 10                 | 34                  | 102                  | ...             | 9                  | 13                | 46/...                        | 46                           | 0.24                    |
| NGC 4386          | SAB0 <sup>0</sup> :      | 27.0              | −19.68 | 140                | 48                  | 74                   | 25              | 134                | 25                | 36/...                        | 36                           | 0.52                    |
| NGC 5338          | SB0 <sup>0</sup> :       | 12.8              | −16.70 | 95                 | 68                  | 76                   | 26              | 125                | 11                | 15/ 15                        | 15                           | 0.46                    |
| NGC 7280          | SAB(r)0 <sup>+</sup>     | 24.3              | −19.16 | 72                 | 48                  | 66                   | ...             | 55                 | 9                 | 29/ 27                        | 21                           | 0.40                    |
| NGC 7743          | (R)SB(s)0 <sup>+</sup>   | 20.7              | −19.49 | 105                | 28                  | 91                   | 45              | 95                 | 31                | 72/ 58                        | 37                           | 0.37                    |
| IC 676            | (R)SB(r)0 <sup>+</sup>   | 19.4              | −18.42 | 15                 | 47                  | 74                   | 15              | 164                | 13                | 40/ 34                        | 18                           | 0.72                    |
| Virgo S0 Galaxies |                          |                   |        |                    |                     |                      |                 |                    |                   |                               |                              |                         |
| NGC 4267          | SB(s)0 <sup>−</sup> ?    | 15.3              | −19.25 | 127                | 25                  | 97                   | 28              | 33                 | 18                | 28/ 26                        | 26                           | 0.21                    |
| NGC 4340          | SB(r)0 <sup>+</sup>      | 15.3              | −18.90 | 95                 | 50                  | 105                  | 53              | 31                 | 39                | 51/ 48                        | 48                           | 0.39                    |
| NGC 4371          | SB(r)0 <sup>+</sup>      | 15.3              | −19.32 | 92                 | 58                  | 119                  | 37              | 167                | 34                | 42/ 40                        | 40                           | 0.26                    |
| NGC 4477          | SB(s)0 <sup>0</sup> :?   | 15.3              | −19.69 | 80                 | 33                  | 114                  | 36              | 12                 | 25                | 45/ 37                        | 37                           | 0.35                    |
| NGC 4596          | SB(r)0 <sup>+</sup>      | 15.3              | −19.63 | 120                | 42                  | 119                  | 40              | 73                 | 52                | 75/ 71                        | 57                           | 0.51                    |
| NGC 4608          | SB(r)0 <sup>0</sup>      | 15.3              | −19.02 | 100                | 36                  | 97                   | 29              | 25                 | 44                | 59/ 57                        | 49                           | 0.48                    |
| NGC 4612          | (R)SAB0 <sup>0</sup>     | 15.3              | −19.01 | 143                | 44                  | 74                   | ...             | 83                 | 17                | 24/ 20                        | 20                           | 0.22                    |
| NGC 4754          | SB(r)0 <sup>−</sup> :    | 16.8              | −19.78 | 23                 | 61                  | 137                  | 36              | 142                | 23                | 27/ 30                        | 27                           | 0.23                    |
| S0/a Galaxies     |                          |                   |        |                    |                     |                      |                 |                    |                   |                               |                              |                         |
| NGC 2681          | (R')SAB(rs)0/a           | 17.2              | −20.20 | 140                | 18                  | 109                  | 27              | 30                 | 50                | 75/ 60                        | 60                           | 0.23                    |
| NGC 4245          | SB(r)0/a                 | 12.0              | −18.28 | 173                | 38                  | 87                   | 30              | 137                | 37                | 56/ 42                        | 42                           | 0.48                    |
| NGC 4643          | SB(rs)0/a                | 18.3              | −19.85 | 55                 | 38                  | 93                   | 54              | 133                | 50                | 69/ 62                        | 62                           | 0.45                    |
| NGC 4665          | SB(s)0/a                 | 10.9              | −18.87 | 120                | 26                  | 114                  | 37              | 4                  | 45                | 99/ 65                        | 65                           | 0.51                    |
| NGC 4691          | (R)SB(s)0/a              | 15.1              | −19.43 | 30                 | 38                  | 85                   | 29              | 82                 | 30                | 69/ 55                        | 45                           | 0.64                    |
| NGC 5701          | (R)SB(rs)0/a             | 21.3              | −19.97 | 45                 | 20                  | 128                  | ...             | 177                | 40                | 58/ 67                        | 58                           | 0.37                    |
| NGC 5750          | SB(r)0/a                 | 26.6              | −19.94 | 65                 | 62                  | 91                   | 22              | 121                | 20                | 24/ 24                        | 22                           | 0.37                    |
| NGC 6654          | (R')SB(s)0/a             | 28.3              | −19.65 | 0                  | 44                  | 79                   | ...             | 17                 | 26                | 47/ 38                        | 38                           | 0.51                    |
| UGC 11920         | SB0/a                    | 18.0              | −19.71 | 50                 | 52                  | 72                   | 38              | 45                 | 26                | 39/...                        | 39                           | 0.51                    |
| Sa Galaxies       |                          |                   |        |                    |                     |                      |                 |                    |                   |                               |                              |                         |
| NGC 718           | SAB(s)a                  | 22.6              | −19.43 | 5                  | 30                  | 71                   | 17              | 152                | 20                | 33/ 30                        | 30                           | 0.23                    |
| NGC 1022          | (R')SB(s)a               | 18.1              | −19.46 | 174                | 24                  | 72                   | 24              | 115                | 19                | 33/ 22                        | 22                           | 0.51                    |
| NGC 2273          | SB(r)a:                  | 27.3              | −20.11 | 50                 | 50                  | 97                   | 30              | 116                | 14                | 17/ 21                        | 17                           | 0.43                    |
| NGC 3185          | (R)SB(r)a                | 17.5              | −18.61 | 140                | 48                  | 71                   | 20              | 114                | 31                | 34/ 32                        | 32                           | 0.58                    |
| NGC 3729          | SB(r)a                   | 16.8              | −19.35 | 170                | 50                  | 85                   | 24              | 26                 | 23                | 27/ 26                        | 26                           | 0.66                    |
| NGC 4045          | SAB(r)a                  | 26.8              | −19.70 | 90                 | 48                  | 81                   | 22              | 18                 | 18                | 22/ 20                        | 20                           | 0.30                    |
| NGC 4314          | SB(rs)a                  | 12.0              | −19.12 | 65                 | 25                  | 125                  | 30              | 146                | 67                | 90/111                        | 80                           | 0.64                    |
| NGC 5377          | (R)SB(s)a                | 27.1              | −20.29 | 25                 | 59                  | 111                  | ...             | 45                 | 58                | 78/...                        | 67                           | 0.66                    |
| Sab Galaxies      |                          |                   |        |                    |                     |                      |                 |                    |                   |                               |                              |                         |
| NGC 3049          | SB(rs)ab                 | 20.2              | −18.65 | 26                 | 51                  | 66                   | 15              | 27                 | 38                | 60/...                        | 38                           | 0.80                    |
| NGC 3368          | SAB(rs)ab                | 10.5              | −20.37 | 172                | 50                  | 228                  | ...             | 115                | 61                | 80/ 75                        | 75                           | 0.40                    |
| NGC 3504          | (R)SAB(s)ab              | 22.3              | −20.29 | 149                | 22                  | 81                   | 22              | 143                | 29                | 45/ 41                        | 34                           | 0.60                    |
| NGC 4151          | (R')SAB(rs)ab:           | 15.9              | −20.70 | 22                 | 20                  | 189                  | 79              | 130                | 65                | 100/ 90                       | 90                           | 0.50                    |
| NGC 4319          | SB(r)ab                  | 23.5              | −19.26 | 135                | 42                  | 89                   | 12              | 152                | 15                | 22/ 17                        | 17                           | 0.51                    |
| NGC 4725          | SAB(r)ab                 | 12.4              | −20.69 | 40                 | 42                  | 321                  | 121             | 50                 | 118               | 130/170                       | 125                          | 0.67                    |
| NGC 6012          | (R)SB(r)ab:              | 26.7              | −19.78 | 45                 | 33                  | 63                   | 42              | 171                | 30                | 99/ 47                        | 36                           | 0.55                    |

$R_{25}$  is one-half of the corrected 25th-magnitude diameter  $D_0$  from RC3, and  $h$  is the outer-disc exponential scale length for galaxies (see Section 3.3). The different measurements of bar size ( $a_e$ ,  $a_{10}$ ,  $a_{\min}$ , and  $L_{\text{bar}}$ ) are discussed in the text (Section 3.1);  $a_e$  and  $L_{\text{bar}}$  can be considered lower and upper limits, respectively, for bar size.  $\epsilon_{\text{max}}$  is the bar's maximum isophotal ellipticity. All disc and bar measurements (except for  $R_{25}$ ) are made from  $R$ -band images, except as noted in the Appendix. Hubble types are from RC3;  $M_B$  is based on distance (usually from LEDA; see text for exceptions) and  $B_{tc}$  from LEDA.

**Table 1.** Continued

| Name        | Type        | Distance<br>(Mpc) | $M_B$  | Outer Disc |            |                 |            | Bar       |              |                          |                         |                   |
|-------------|-------------|-------------------|--------|------------|------------|-----------------|------------|-----------|--------------|--------------------------|-------------------------|-------------------|
|             |             |                   |        | PA<br>(°)  | $i$<br>(°) | $R_{25}$<br>(″) | $h$<br>(″) | PA<br>(°) | $a_e$<br>(″) | $a_{\min}/a_{10}$<br>(″) | $L_{\text{bar}}$<br>(″) | $\epsilon_{\max}$ |
| Sb Galaxies |             |                   |        |            |            |                 |            |           |              |                          |                         |                   |
| NGC 2712    | SB(r)b:     | 26.5              | -19.88 | 10         | 59         | 87              | 20         | 32        | 22           | 27/ 27                   | 24                      | 0.64              |
| NGC 3351    | SB(r)b      | 10.0              | -19.94 | 13         | 56         | 222             | ...        | 112       | 52           | 68/ 68                   | 58                      | 0.42              |
| NGC 3485    | SB(r)b:     | 20.0              | -19.03 | 5          | 26         | 69              | 22         | 45        | 20           | 35/ 34                   | 24                      | 0.64              |
| NGC 3507    | SB(s)b      | 14.2              | -19.21 | 90         | 27         | 102             | 25         | 112       | 26           | 37/ 33                   | 29                      | 0.52              |
| NGC 3982    | SAB(r)b:    | 18.0              | -19.63 | 17         | 30         | 70              | ...        | 10        | 4            | 5/ 6                     | 5                       | 0.25              |
| NGC 4037    | SB(rs)b:    | 13.5              | -17.79 | 150        | 32         | 75              | 34         | 11        | 27           | 38/ 42                   | 33                      | 0.62              |
| NGC 4102    | SAB(s)b?    | 14.4              | -19.22 | 38         | 55         | 91              | ...        | 67        | 10           | 15/...                   | 15                      | 0.45              |
| NGC 4699    | SAB(rs)b    | 18.9              | -21.37 | 37         | 42         | 114             | 13         | 50        | 13           | 19/ 16                   | 16                      | 0.46              |
| NGC 4995    | SAB(r)b     | 23.6              | -20.41 | 93         | 47         | 74              | 17         | 26        | 16           | 24/ 22                   | 19                      | 0.34              |
| NGC 5740    | SAB(rs)b    | 22.0              | -19.67 | 161        | 60         | 89              | 17         | 123       | 12           | 14/ 22                   | 14                      | 0.47              |
| NGC 5806    | SAB(s)b     | 19.2              | -19.67 | 166        | 58         | 93              | 30         | 175       | 37           | 95/ 82                   | 38                      | 0.62              |
| NGC 5832    | SB(rs)b?    | 9.9               | -17.15 | 45         | 55         | 111             | 21         | 159       | 26           | 33/ 34                   | 30                      | 0.29              |
| NGC 5957    | (R')SAB(r)b | 26.2              | -19.36 | 100        | 15         | 85              | ...        | 97        | 24           | 37/ 31                   | 27                      | 0.53              |
| NGC 7177    | SAB(r)b     | 16.8              | -19.79 | 83         | 48         | 93              | 17         | 13        | 10           | 14/ 13                   | 11                      | 0.39              |
| IC 1067     | SB(s)b      | 22.2              | -18.82 | 110        | 36         | 64              | 15         | 151       | 19           | 23/ 23                   | 19                      | 0.64              |
| UGC 3685    | SB(rs)b     | 26.8              | -19.51 | 119        | 31         | 99              | 45         | 131       | 25           | 35/ 30                   | 27                      | 0.59              |

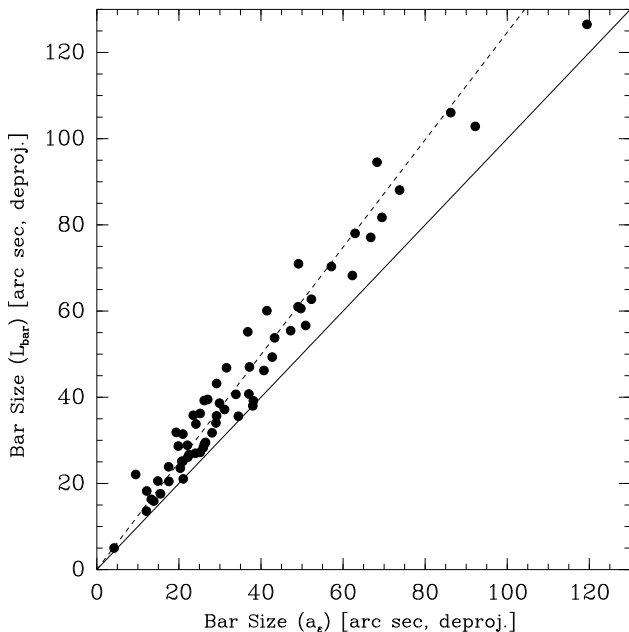


**Figure 2.** Correlation between two deprojected measurements of bar semimajor axis – semimajor axis at maximum isophotal ellipticity ( $a_e$ ) and bar length ( $L_{\text{bar}}$ ; see text for definition) – for S0–Sb galaxies. The dashed line indicates the mean ratio of the two measurements:  $L_{\text{bar}} = 1.25a_e$ .

ages, and the position angle determined from the isophotes and unsharp masking is preferred to the ellipse-fit position angle if the two differ by more than a couple of degrees.

Finally, the inclination and line-of-nodes of the galaxy discs need to be determined. The easiest approach is to use the RC3 axis ratios and position angles and assume that the outer disc is circular. Unfortunately, this is by no means the most accurate way, especially for early-type barred galaxies. This is because the RC3 axis ratios sometimes reflect bar-related features such as inner rings, lenses, and outer

rings, which are more common in early-type disc galaxies and which are *not* always intrinsically circular (Buta 1986, 1995). So I determined the outer disc orientation, where possible, using kinematic information (e.g., H I maps) and/or isophotes at diameters larger than  $D_{25}$ . For the WIYN Sample galaxies, I use the values from Erwin & Sparke (2003), which were determined using this approach (certain exceptions based on more recent data are mentioned in the Appendix). Details for the Virgo S0 and the Sab–Sb galaxies are given in the Appendix.

### 3.2 Measuring the Shapes of Bars

Another way to define a bar is by its “strength.” This too lacks an obvious, universally agreed-upon definition. The simplest way to measure a bar’s strength is to measure its *shape*, usually reduced to measuring its “ellipticity.” For theorists, this often means the ellipticity of the bar itself (e.g., that of a Ferrers ellipsoid), but for observers – lacking the ability to unambiguously isolate the bar from other galactic components – it usually means measuring the semiminor axis of the *isophote* defined by the bar length (usually  $a_e$ ) and comparing it with the semimajor axis. This is approximately the method used by Martin (1995) to define bar strengths, and also by Shlosman et al. (2000) and Laine et al. (2002) for fitted ellipses defining bars. For comparison, if no other reason, it makes sense to do the same.

A more complex approach, which attempts to estimate the non-axisymmetric gravitational influence of the bar, is that of Buta & Block (2001). Unfortunately, this generally requires near-IR images, and assumes that the entire galaxy is flat with a constant scale height. For bars in late-type galaxies, where the bulge is small or even absent, this is probably reasonable; but for early-type galaxies, large bulges – and possibly multiple disc components with different thicknesses – make this a questionable assumption. (More recently, Laurikainen et al. 2004 have included a spherical bulge component in the modeling process, which alleviates some of the problems.) Happily, Laurikainen et al. (2002)

find that the bar strength measured this way correlates quite well with bar ellipticity.

### 3.3 Measuring the Sizes of Discs

Galaxies come in many sizes, and what might be a large bar in one galaxy would be small in another. Thus, although absolute measurements of bars size (in kpc) are useful, we also need some kind of relative measurement. What should we compare bar sizes with?

The simplest approach is to follow Elmegreen & Elmegreen (1985) and Martin (1995): compare the bar size to the optical disc size  $D_{25}$ , which is available for all the galaxies. Since I measure bar semimajor axes, I use  $R_{25} = D_{25}/2$  for the disc size. To be consistent with Martin’s measurements, I use the  $D_0$  values from RC3, which are corrected for inclination (usually a very small effect) and for Galactic extinction.

Another useful measurement is the exponential scale length of the disc. Combes & Elmegreen (1993) argued that bars in late-type galaxies should extend to approximately one disc scale length, and Laine et al. (2002) suggested that the correlation they observed between bar size ( $a_e$ ) and  $D_{25}$  implied that bars “extend to a fixed number of radial scale lengths in the disk.” Bar sizes in terms of disc scale lengths are also much easier to compare with simulations, since exponential scale lengths for  $n$ -body discs are easily measured.

For those galaxies in which an outer exponential disc can be identified, I derive its slope by fitting the region *outside the bar*, using an azimuthally averaged surface-brightness profile.<sup>5</sup> This is the classic approach of “marking the disc” by eye. In principle, more accurate scale lengths might be derived by performing a bulge-disc decomposition, so that the contribution of bulge light to the outer disc profile is accounted for. I do *not* attempt this, however, since many of these galaxies are strongly barred and/or contain luminous central structures apart from the bulge (secondary bars, inner discs, or nuclear rings). In extreme cases, these non-bulge components can dominate the interior light (Erwin et al. 2003), and attempting to fit them with, e.g., a de Vaucouleurs or Sérsic profile could assign too much light at large radii to the “bulge” and distort the disc fit. Since I am deliberately fitting only the region outside the bar, the effect of bulge light in most cases is minimized. In any event, de Jong (1996) found that the change in derived scale length between marking the disc and more sophisticated decomposition techniques was typically only a few percent. A comparison of my disc scale lengths with those of Baggett et al. (1998), which were obtained via bulge-disc decompositions, show a similarly small variation; see Section 3.4 below. Details for unusual cases are provided in the Appendix, along with notes for galaxies where severely non-exponential outer discs prevented determining an exponential scale length.

Another reason for fitting the outer disc only is shown in Figure 3. Although it is sometimes argued that bars vanish from the surface-brightness profile when it is averaged, leaving behind only the underlying exponential disc (e.g. Elmegreen & Elmegreen 1985; Ohta et al. 1990), this is not

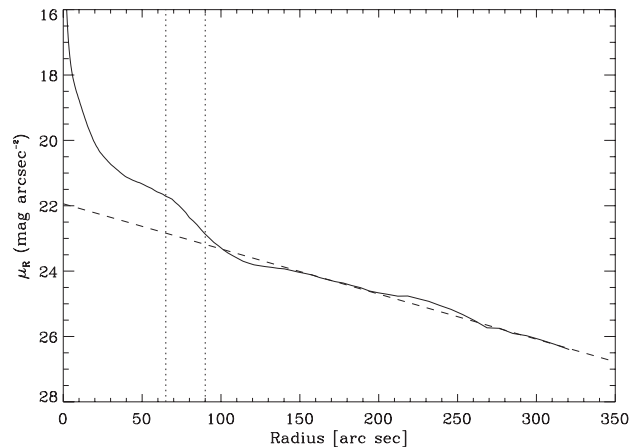


**Figure 3.** Azimuthally averaged  $R$ -band profile for NGC 4151. The vertical, short-dashed lines indicate deprojected bar-size measurements  $a_e$  and  $L_{\text{bar}}$ ; the diagonal, long-dashed line is an exponential fit to the disc region outside the bar ( $r > 145''$ , excluding the ring excess at  $r \sim 200$ – $260''$ ). Note the excess light at  $r \sim 40$ – $100''$ , which is primarily due to the bar.

always true: the bar can sometimes appear as a clear, significant excess above the (outer) exponential profile (see also de Jong 1996). None the less, if we exclude the bar region and any excess just outside it, we can still distinguish an unambiguous outer exponential profile in such galaxies (see Erwin, Pohlen, & Beckman, in preparation, for details).

However, in other galaxies the outer disc does not have a single exponential profile. For 16 galaxies, the profile outside the bar is what Freeman (1970) termed a “Type II” profile: it is divided into *two* (usually) exponential zones: a shallow inner zone and a steeper outer zone (see Figure 4 for an example). In such cases, it is not at all clear which of the two zones – if either – should be considered the “true” outer disc. In at least some cases (e.g., NGC 2859, 3412, 2962, 5701, and 6654), the inner zone is extremely narrow and/or shallow in slope, or even *increasing* in brightness with radius. The simplest solution is to ignore these more extreme “outer” Type II profiles. (Five other galaxies have Type II profiles with a deficit *inside* the bar, so there is still a single exponential profile *outside* the bar; these are similar to profiles produced in some  $n$ -body simulations – e.g., Valenzuela & Klypin 2003).

There are additional galaxies where the surface brightness profile at large radii is shallower than that of disc immediately outside the bar; these are the “Type III” or “anti-truncation” profiles discussed in Erwin et al. (2005). Because these galaxies *do* have an extended, well-defined exponential zone outside the bar, I include their scale length measurements. The presence of extended light at large radius may contribute to a subtle selection effect, which I discuss in Section 4.1.

### 3.4 Comparing Measurements: Early- and Late-Type Galaxies

The bar sizes of the S0–Sb galaxies are measured using a combination of ellipse fits and direct inspection of  $R$ -band images, supplemented by near-IR images when dust is strong. The bar sizes of Martin (1995), on the other hand,

<sup>5</sup> That is, a profile obtained with concentric, similar ellipses using the “Outer Disc” position angle and ellipticity from Table 1.

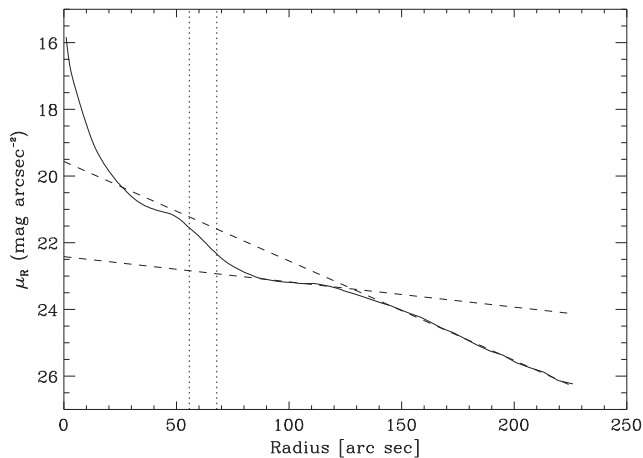


**Figure 4.** As for Figure 3, but showing the profile of NGC 3945, which has *two* exponential zones outside the bar (an example of a Freeman Type II profile). Because there is no single, well-defined exponential zone in such galaxies, I do not compute bar sizes relative to disc scale lengths for them.

are based on measurements made on blue photographic prints. How consistent are these measurements? And which of my two measurements ( $a_e$  and  $L_{\text{bar}}$ ) is a better match to Martin’s single bar-size measurement?

Unfortunately, there are almost no galaxies in common between the two samples, even among the Sb subset (the three shared galaxies are NGC 3351, 3485, and 4725, where Martin finds  $a = 46''$ ,  $18''$ , and  $109''$ , respectively; these values are only slightly smaller than my  $a_e = 52''$ ,  $23''$ , and  $118''$ ). This makes it difficult to tell which of the two,  $a_e$  and  $L_{\text{bar}}$ , is a better match to Martin’s visual estimates. Fortunately, Martin compared his measurements with the visual bar-size measurements of Kormendy (1979) – and there *are* numerous overlaps between Kormendy’s sample and mine.<sup>6</sup> In Figure 5, I compare  $a_e$  and  $L_{\text{bar}}$  measurements with those of Kormendy for galaxies in common. Kormendy’s measurements generally sit in between  $a_e$  and  $L_{\text{bar}}$ ; in fact, the best agreement is with the *mean* of  $a_e$  and  $L_{\text{bar}}$ , which I will refer to as  $L_{\text{avg}}$ . Since Martin found excellent agreement between Kormendy’s measurements and *his* for galaxies in common between *their* samples, this suggests that  $L_{\text{avg}}$  is a reasonable match to Martin’s bar lengths. (The results discussed below do not change significantly if I compare Martin’s measurements with  $a_e$  instead.)

The disc scale lengths for the galaxies from Martin (1995), when available, are taken from Baggett et al. (1998, hereafter BBA98). This is the only study with large numbers of scale lengths which overlaps significantly with both the early-type galaxies in my sample *and* the later-type galaxies in Martin’s sample. The BBA98 fits differ from mine in using major-axis cuts from V-band photographic images, and in using bulge-disc decompositions with an optional “hole” in the disc. Since the “bulge” component (i.e., the central excess over the exponential disc, which BBA98 model with a de Vaucouleurs profile) in late-type galaxies is generally

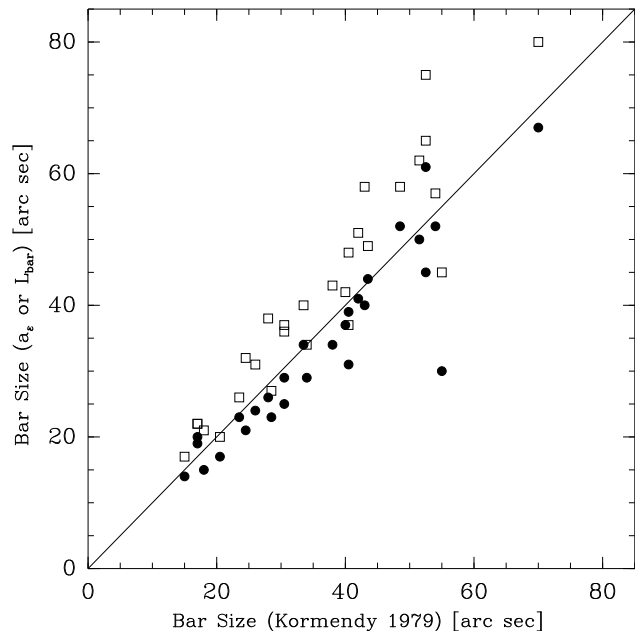


**Figure 5.** Comparison of observed (i.e., projected) bar size measurements between this study and Kormendy (1979):  $a_e$  values are shown with filled circles,  $L_{\text{bar}}$  with open boxes.

smaller and less luminous than in earlier types, the effect on the disc fit is reduced.

The optional hole in their disc model, which is intended to account for Type II profiles, introduces a new problem, however: it forces the bulge component to account for all the inner light (including, e.g., the inner part of the disc and the bar). Since the bulge model is not truncated, it ends up contributing more light at large radii than the true bulge probably does, and can thus distort the disc fit. The “disc with hole” fits also obviously indicate possible Type II profiles, which, as noted in Section 3.3, are problematic for estimating scale lengths. However, because they use major-axis cuts rather than azimuthally averaged profiles, at least some of their Type II profiles turn out to be Type I when azimuthally averaged. This generally happens when the bar is oriented at an intermediate angle or perpendicular to the major-axis cut, and probably signals the transition between the outer disc and, e.g., a lens in which the bar is embedded (e.g., NGC 2787; see Erwin, Pohlen, & Beckman, in preparation, and also Ohta et al. 1990).

To evaluate how well the BBA98 disc scale lengths compare with mine, Figure 6 plots scale lengths for galaxies in common between this study and BBA98. There is a fair amount of scatter, but the agreement is generally good *if* I reject BBA98 scale lengths when the hole radius is more than twice the scale length. This criterion would also reject 6 of the 9 Type II profiles from my sample which are also in BBA98 (not plotted), so I use the BBA98 scale lengths only when their fit has no hole or a hole with radius  $< 2h$ .

The comparison in Figure 6 is also useful as a test of how well scale lengths measured directly from the profile (“marking the disc”) compare with those derived from a bulge-disc decomposition, as done by BBA98. Except for cases where BBA98 used very large holes in their discs (large open symbols), the agreement is rather good. There is a very

<sup>6</sup> There is not enough information about bar orientation in Kormendy’s Table 1 to allow reliable deprojections of his bar sizes; in addition, his sample is limited to SB galaxies.

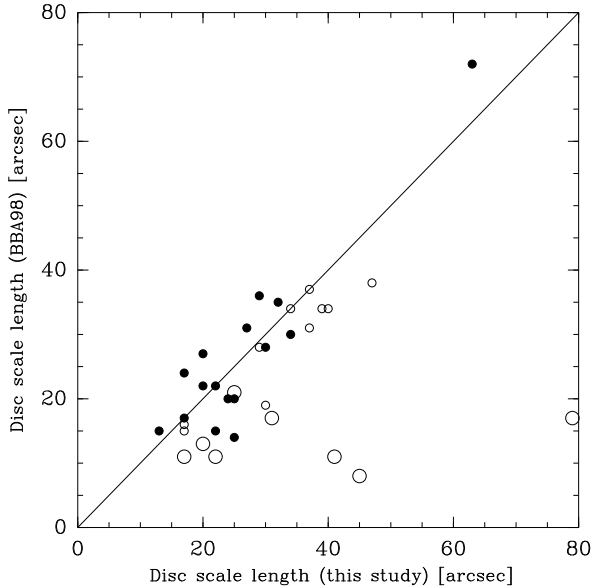


**Figure 6.** Comparison of exponential disc scale lengths for galaxies in common between this study and BBA98 (Baggett et al. 1998). Different symbols indicate different types of fits from Baggett et al.: filled circles are standard discs (no holes), small hollow circles are fits using discs with holes having radii  $< 2$  times disc scale length  $h$ , and large hollow circles are fits with large holes ( $r_{\text{hole}} > 2h$ ). The agreement is generally good except when the BBA98 fits have large holes.

weak systematic trend: my scale lengths are on average 4% larger than the BBA98 scale lengths. But since the *relative* scatter (absolute value) is 17%, this is not a very significant difference.

Figure 7 shows the run of  $R_{25}/h$  versus Hubble type for the combined samples. In general, the early-type galaxies have  $R_{25} \sim 3h$ , while Sb and later-type galaxies have  $R_{25} \sim 4h$ , presumably because their discs have more younger stars, and are thus bluer and brighter. As I will show in Section 4.1, this has some implications for relative bar sizes.

#### 4 BARS SIZES, STRENGTHS, AND HUBBLE TYPE

In this section I look at how bar sizes, in absolute and relative terms, vary with Hubble type and with bar strength. I also investigate whether and to what degree the size of bars correlates with galaxy size and luminosity, and with bar strength. I begin by discussing the S0–Sb bars from my sample in isolation, both because my sample is more consistent and complete than that of Martin (1995) and because I measured *two* bar sizes ( $a_e$  and  $L_{\text{bar}}$ ) versus the single measurement of Martin. I then add in the later types of Martin’s sample and look at the run of bar sizes along the Hubble sequence from S0–Sd, and finally examine how bar size relates to bar strength.

##### 4.1 Bars in Early-Type Galaxies

Figure 8 shows absolute bars sizes as a function of Hubble type for the S0–Sb galaxies; Figures 9 and 10 show the run of

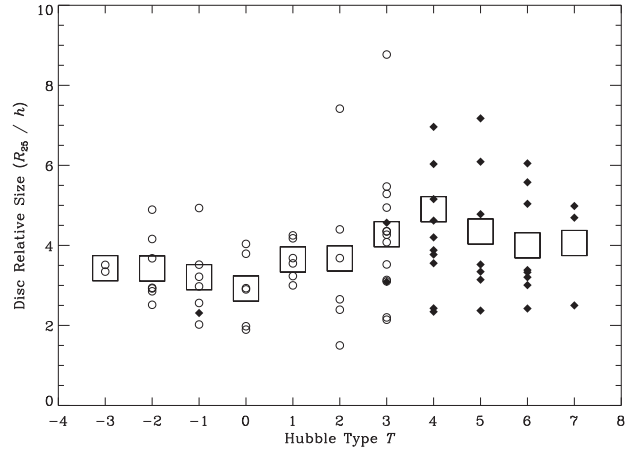


**Figure 7.** Isophotal disc size ( $R_{25}$ ) in terms of the exponential scale length  $h$ , as a function of Hubble type. Galaxies from my sample are shown with open circles, while galaxies from Martin (1995) meeting the same selection criteria are shown with filled diamonds; mean values for each Hubble type are indicated by the large boxes.

bar sizes relative to  $R_{25}$  and the disc scale length  $h$ . Table 2 shows mean bar sizes for different galaxy types, and Tables 3 and 4 show the strength of different correlations between bar sizes and galaxy properties.

Bar and disc sizes are well correlated for these galaxies; the correlations between bar sizes and outer-disc scale length are equally good. In fact, when only those galaxies with measured scale lengths are considered (Table 4), the *strongest* correlation is with the disc scale length (this may be biased by the Sb galaxies; see below). There is also a correlation between bar size and blue luminosity, as first noted by Kormendy (1979); however, it is clearly not as strong as the correlations with  $h$  and  $R_{25}$ . This is reasonable, since bars are disc phenomena and  $M_B$  can include variable contributions from the bulge; in addition, it may be more affected by variations in star formation and dust extinction.

The correlation between bar size and scale length is strongest for Sb galaxies (Table 4), but the correlations with  $R_{25}$  and  $M_B$  are noticeably weaker. The Sb galaxies are also odd in having bars which are smaller in absolute and  $R_{25}$ -relative size (Figures 8 and 9) – and yet almost the *same* size relative to the disc scale length (Figure 10).

This curious situation may partly be due to higher levels of recent star formation in the Sb and later galaxies, which makes their discs brighter and thus larger – in blue isophotal size – for a given scale length (see Figure 7). For the Sb galaxies in my sample,  $R_{25}/h = 3.9 \pm 1.1$  ( $3.9 \pm 1.0$  if Sb galaxies from Martin [1995] are included), versus  $3.2 \pm 0.9$  for the S0–Sab galaxies. For the combined Sb–Sd galaxies, the mean size is  $R_{25}/h = 4.3 \pm 1.7$ . Kolmogorov–Smirnov (K–S) tests suggest that there is indeed a significant difference in relative disc size between early and late types, starting with the Sb galaxies: the Sb–Sd  $R_{25}/h$  ratios are inconsistent with those of S0–Sab galaxies ( $P = 0.012$ ).

Thus, my selection criterion of  $D_{25} \geq 2.0'$  means that the Sb subsample includes galaxies with smaller  $h$  – and thus bars with smaller absolute sizes – than the earlier Hubble types: mean  $h = 2.5 \pm 1.7$  kpc for Sb galaxies versus  $3.0 \pm 1.6$  kpc for S0–Sab galaxies. If the star formation in Sb and later

**Table 2.** Mean Bar Sizes for S0–Sb Galaxies

| Types                             | Mean $a_\epsilon$ | Mean $L_{\text{bar}}$ |
|-----------------------------------|-------------------|-----------------------|
| Absolute Size (kpc)               |                   |                       |
| All S0–Sb                         | $3.0 \pm 1.6$     | $3.7 \pm 1.9$         |
| All S0                            | $2.7 \pm 1.6$     | $3.6 \pm 1.8$         |
| S0/a                              | $3.6 \pm 1.2$     | $4.8 \pm 1.4$         |
| Sa                                | $3.6 \pm 2.2$     | $4.2 \pm 2.6$         |
| Sab                               | $4.3 \pm 1.7$     | $5.0 \pm 2.0$         |
| Sb                                | $2.2 \pm 1.1$     | $2.5 \pm 1.1$         |
| SB                                | $3.2 \pm 1.6$     | $3.8 \pm 1.8$         |
| SAB                               | $2.7 \pm 1.7$     | $3.5 \pm 2.0$         |
| Fraction of Disc Size $R_{25}$    |                   |                       |
| All S0–Sb                         | $0.34 \pm 0.13$   | $0.42 \pm 0.15$       |
| All S0                            | $0.32 \pm 0.13$   | $0.43 \pm 0.13$       |
| S0/a                              | $0.43 \pm 0.11$   | $0.57 \pm 0.12$       |
| Sa                                | $0.39 \pm 0.15$   | $0.46 \pm 0.16$       |
| Sab                               | $0.39 \pm 0.13$   | $0.46 \pm 0.14$       |
| Sb                                | $0.27 \pm 0.11$   | $0.31 \pm 0.12$       |
| SB                                | $0.37 \pm 0.13$   | $0.45 \pm 0.15$       |
| SAB                               | $0.27 \pm 0.11$   | $0.37 \pm 0.14$       |
| Fraction of Disc Scale Length $h$ |                   |                       |
| All S0–Sb                         | $1.27 \pm 0.52$   | $1.51 \pm 0.56$       |
| All S0                            | $1.16 \pm 0.43$   | $1.44 \pm 0.42$       |
| S0/a                              | $1.37 \pm 0.42$   | $1.70 \pm 0.44$       |
| Sa                                | $1.43 \pm 0.82$   | $1.63 \pm 0.96$       |
| Sab                               | $1.30 \pm 0.72$   | $1.46 \pm 0.64$       |
| Sb                                | $1.20 \pm 0.49$   | $1.38 \pm 0.58$       |
| SB                                | $1.27 \pm 0.55$   | $1.50 \pm 0.58$       |
| SAB                               | $1.29 \pm 0.41$   | $1.54 \pm 0.49$       |

galaxies is also more *variable* than in earlier types, then the weaker correlations of Sb bar size with  $R_{25}$  and  $M_B$  make sense as well.

An additional possible effect is the existence of galaxies with excess light at larger radii, relative to the outward projection of the exponential disc profile. These are the Type III profiles of Erwin et al. (2005), and they are, in this sample at least, especially common in both Sb galaxies and S0 galaxies (31% and 32%, respectively, of those Hubble types, compared with 13% of the S0/a–Sab galaxies). Again, if we assume that bar size scales most strongly with inner-disc  $h$ , then a diameter-limited selection will preferentially include S0 and Sb galaxies with smaller disc scale lengths and smaller bars, when compared with S0/a–Sab galaxies in the same sample.

Table 2 *does* show a slight tendency for both S0 and Sb bars to be smaller in size relative to disc scale length, but this is not statistically significant: for example, a K-S test gives  $P = 76\text{--}87\%$  that Sb and S0/a–Sab bar sizes relative to  $h$  come from the same parent population. So despite what Figures 8 and 9 seem to suggest, it is not clear that S0 and Sb bars are really smaller than the bars in S0/a–Sab galaxies. If size relative to disc scale length is the most reliable measuring stick, then there is no significant difference in bar size over the range S0–Sb.

Although most of the galaxies in my sample are from the field, I did include eight S0 galaxies from the Virgo Cluster. Do Virgo S0’s have different bar properties from field S0’s? The Virgo lenticulars *do* tend to have slightly larger bars

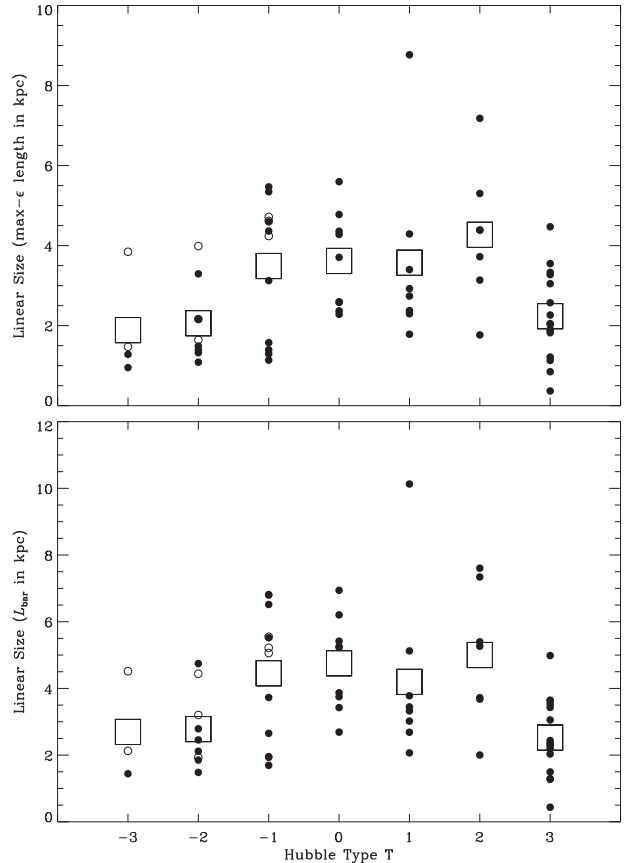


**Figure 8.** Deprojected sizes of S0–Sb bars in absolute terms (semimajor axis in kpc), using maximum-ellipticity length  $a_\epsilon$  (top) and  $L_{\text{bar}}$  (bottom). Virgo Cluster S0 galaxies are indicated by hollow circles, with filled circles for field galaxies. The mean values for each Hubble type are indicated by the large boxes.

than the field S0’s (e.g., mean  $a_\epsilon/R_{25} = 0.41 \pm 0.15$  versus  $0.28 \pm 0.09$ ; mean  $a_\epsilon/h = 1.25 \pm 0.49$  versus  $1.06 \pm 0.39$ ). However, none of these differences is statistically significant: K-S tests give probabilities of 9–88% for the field and Virgo S0 bar sizes being drawn from the same parent population.

## 4.2 Bar Sizes in Later-Type Galaxies and the Hubble Sequence

When galaxies from the sample of Martin (1995, see Section 3.4) are added to the S0–Sb galaxies, the Hubble sequence coverage extends down to Sd galaxies. Figures 11–13 and Table 5 show bar sizes for this combined set of galaxies. As noted by earlier studies (Elmegreen & Elmegreen 1985; Martin 1995; Laurikainen et al. 2002), there is a clear tendency for bars in later Hubble types to be smaller; this is true using both relative-size measurements *and* absolute sizes.

Crudely speaking, one can divide the Hubble sequence into two zones, plus a transition region. Bars in S0–Sb galaxies are clearly larger than bars in late-type (Sc–Sd) galaxies. On average, the early-type bars are  $\approx 2.2\text{--}2.7$  times as large as late-type bars. The K-S probabilities that S0–Sb bars come from the same parent population as Sc–Sd bars are  $7.9 \times 10^{-11}$  for  $L_{\text{avg}}$  in kpc,  $3.3 \times 10^{-15}$  for  $L_{\text{avg}}/R_{25}$ , and  $5.1 \times 10^{-6}$  for  $L_{\text{avg}}/h$ ; so the result is quite robust (to

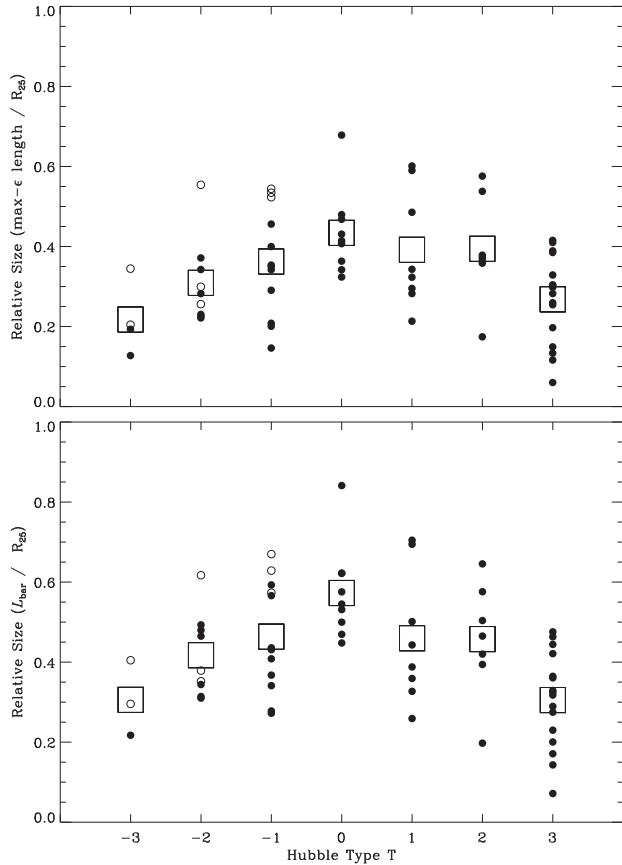


**Figure 9.** As for Figure 8, but now showing sizes of bars relative to disc radius  $R_{25}$ .

put it mildly). It is worth mentioning that Martin (1995) noted that some bars in his sample could not be measured because “the inner parts of the disc were overexposed.” This indicates a possible bias against very small bars in Martin’s final set of measurements, which apply to later-type galaxies, so the difference could be even greater.

But where does the transition take place, and how abrupt is it? Figures 11 and 12 make it appear that Sb and Sbc galaxies are a continuation of later-type galaxies: in particular, they have some very small bars ( $L_{\text{avg}} \lesssim 1$  kpc and  $\lesssim 0.2R_{25}$ ) not found in earlier types. However, this continuity may be partly an illusion. As discussed in the previous section, the combination of large  $R_{25}/h$  values for Sb galaxies (mean =  $3.9 \pm 1.0$ ) and diameter-limited selection leads to the inclusion of Sb galaxies with smaller disc scale lengths than is the case for the earlier Hubble types; since bar size correlates with scale length for these galaxies, this leads to the inclusion of Sb bars with smaller absolute and  $R_{25}$ -relative sizes. This is partly the case for Sbc galaxies as well: their mean  $R_{25}/h$  is  $4.9 \pm 2.5$ , in comparison with  $4.1 \pm 1.4$  for the Sc–Sd galaxies (there is little variation in  $R_{25}/h$  among the latter types; see Figure 7).

So once again the best picture is probably had by looking at bar sizes relative to the disc scale length (Figure 13). This shows that Sb bars *are* distinct from Sc–Sd bars, and that they are largely indistinguishable from bars in earlier Hubble types, as I argued in the previous section. The transition point between the early- and late-type regimes is thus

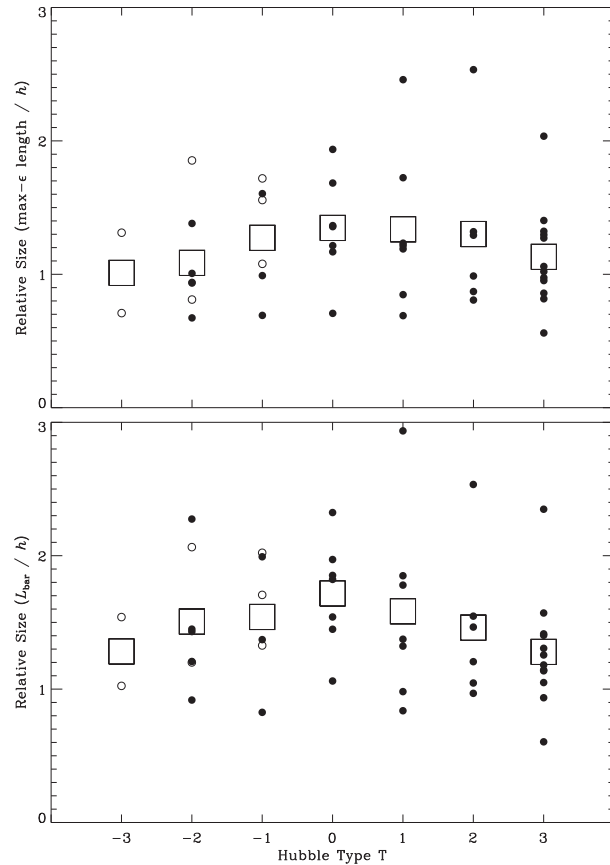


**Figure 10.** As for Figure 8, but now showing sizes of bars relative to the outer-disc exponential scale length  $h$ .

the Sbc galaxies: their average bar sizes are intermediate, but they include both bars as large as those in earlier types *and* bars shorter than  $0.5h$ , common in Sc–Sd galaxies but absent in the early types.

An additional, significant difference between bars in early- and late-type galaxies is the weakness or absence of correlations between bar size and other galaxy properties for the late-type galaxies. Table 6 compares the various correlations between bar size. In all cases, the later galaxy types have weaker bar-size correlations – in fact, for Sc–Sd galaxies, the correlation with  $M_B$  is no longer statistically significant, and there is apparently *no* correlation between bar size and disc scale length!

It is interesting – and perhaps suspicious – that these differences are primarily between galaxies in my sample (Sb and earlier) and the later types of Martin’s (1995) sample. Since the two sample have bar (and disc scale length) measurements from different sources, some of the dichotomy could be due to varying measurement techniques or biases. But at least some of it is probably real. Table 7 repeats the correlation analysis using only galaxies from Martin – including galaxies with  $V > 2000$  km s<sup>−1</sup> in order to boost the number of Sb galaxies. The table shows the same trends as Table 6, including the strong correlation of bar size with disc scale length for Sb galaxies. This suggests that the pronounced absence of almost any correlations in Sc–Sd galaxies between bar size and disc size or galaxy luminosity is probably real. As I show in the next section, this result appears

**Table 3.** Correlations for S0–Sb Galaxies

| Correlation                   | Pearson $r$ ( $P$ )            | Spearman $r_s$ ( $P$ )         |
|-------------------------------|--------------------------------|--------------------------------|
| All S0–Sb Galaxies            |                                |                                |
| $a_e$ vs. $R_{25}$            | 0.73 ( $9.4 \times 10^{-12}$ ) | 0.69 ( $3.9 \times 10^{-10}$ ) |
| $L_{\text{bar}}$ vs. $R_{25}$ | 0.72 ( $1.4 \times 10^{-11}$ ) | 0.68 ( $6.0 \times 10^{-10}$ ) |
| $a_e$ vs. $M_B$               | −0.46 ( $1.3 \times 10^{-4}$ ) | −0.51 ( $1.5 \times 10^{-5}$ ) |
| $L_{\text{bar}}$ vs. $M_B$    | −0.48 ( $6.4 \times 10^{-5}$ ) | −0.53 ( $7.8 \times 10^{-6}$ ) |
| S0 Galaxies                   |                                |                                |
| $a_e$ vs. $R_{25}$            | 0.81 ( $1.8 \times 10^{-6}$ )  | 0.75 ( $2.3 \times 10^{-5}$ )  |
| $L_{\text{bar}}$ vs. $R_{25}$ | 0.84 ( $2.2 \times 10^{-7}$ )  | 0.84 ( $3.0 \times 10^{-7}$ )  |
| $a_e$ vs. $M_B$               | −0.58 (0.0029)                 | −0.59 (0.0025)                 |
| $L_{\text{bar}}$ vs. $M_B$    | −0.62 (0.0013)                 | −0.64 ( $8.1 \times 10^{-4}$ ) |
| S0/a–Sab Galaxies             |                                |                                |
| $a_e$ vs. $R_{25}$            | 0.70 ( $1.2 \times 10^{-4}$ )  | 0.64 ( $7.2 \times 10^{-4}$ )  |
| $L_{\text{bar}}$ vs. $R_{25}$ | 0.69 ( $1.7 \times 10^{-4}$ )  | 0.65 ( $5.8 \times 10^{-4}$ )  |
| $a_e$ vs. $M_B$               | −0.59 (0.0026)                 | −0.64 ( $7.7 \times 10^{-4}$ ) |
| $L_{\text{bar}}$ vs. $M_B$    | −0.64 ( $8.5 \times 10^{-4}$ ) | −0.66 ( $4.5 \times 10^{-4}$ ) |
| Sb Galaxies                   |                                |                                |
| $a_e$ vs. $R_{25}$            | 0.61 (0.013)                   | 0.58 (0.019)                   |
| $L_{\text{bar}}$ vs. $R_{25}$ | 0.60 (0.015)                   | 0.56 (0.025)                   |
| $a_e$ vs. $M_B$               | −0.05 (0.84)                   | −0.15 (0.59)                   |
| $L_{\text{bar}}$ vs. $M_B$    | −0.05 (0.85)                   | −0.15 (0.58)                   |

Correlations between bar size ( $a_e$ ,  $L_{\text{bar}}$ ) and galaxy size ( $R_{25}$ ) and blue luminosity ( $M_B$ ). For each correlation coefficient, the probability of the correlation being purely due to chance is given in parentheses.

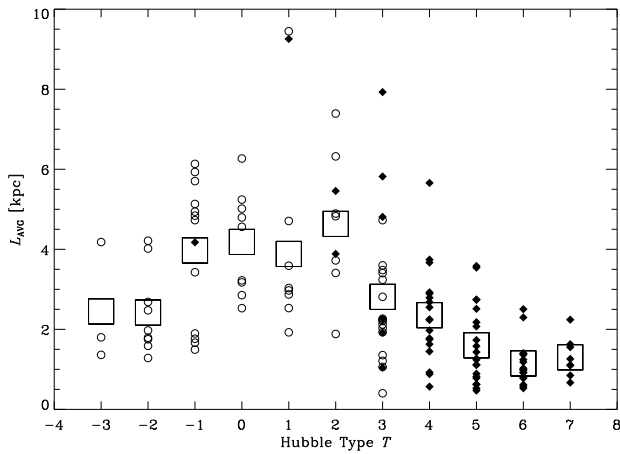


**Figure 11.** Sizes of S0–Sdm bars in absolute terms (kpc), combining my sample (circles) with galaxies from Martin (1995) meeting the same selection criteria (diamonds). All bar lengths are deprojected; as explained in the text, I use the average of  $a_e$  and  $L_{\text{bar}}$  for galaxies in my sample as the best match to Martin’s bar measurements. Mean values for each Hubble type (using galaxies from my sample only for S0–Sb) are indicated by the large boxes.

**Table 4.** Correlations for S0–Sb Galaxies with Measured Scale Lengths

| Correlation                   | Pearson $r$ ( $P$ )           | Spearman $r_s$ ( $P$ )         |
|-------------------------------|-------------------------------|--------------------------------|
| All S0–Sb Galaxies            |                               |                                |
| $a_e$ vs. $h$                 | 0.73 ( $6.4 \times 10^{-9}$ ) | 0.72 ( $10.0 \times 10^{-9}$ ) |
| $L_{\text{bar}}$ vs. $h$      | 0.75 ( $1.8 \times 10^{-9}$ ) | 0.75 ( $1.8 \times 10^{-9}$ )  |
| $a_e$ vs. $R_{25}$            | 0.63 ( $2.5 \times 10^{-6}$ ) | 0.53 ( $1.2 \times 10^{-4}$ )  |
| $L_{\text{bar}}$ vs. $R_{25}$ | 0.59 ( $1.5 \times 10^{-5}$ ) | 0.48 ( $5.8 \times 10^{-4}$ )  |
| $a_e$ vs. $M_B$               | −0.40 (0.006)                 | −0.39 (0.0071)                 |
| $L_{\text{bar}}$ vs. $M_B$    | −0.42 (0.0032)                | −0.41 (0.0044)                 |
| S0 Galaxies                   |                               |                                |
| $a_e$ vs. $h$                 | 0.69 (0.0044)                 | 0.71 (0.0028)                  |
| $L_{\text{bar}}$ vs. $h$      | 0.72 (0.0024)                 | 0.80 ( $3.4 \times 10^{-4}$ )  |
| $a_e$ vs. $R_{25}$            | 0.70 (0.004)                  | 0.69 (0.0048)                  |
| $L_{\text{bar}}$ vs. $R_{25}$ | 0.74 (0.0016)                 | 0.76 ( $9.1 \times 10^{-4}$ )  |
| $a_e$ vs. $M_B$               | −0.47 (0.074)                 | −0.43 (0.11)                   |
| $L_{\text{bar}}$ vs. $M_B$    | −0.55 (0.032)                 | −0.54 (0.038)                  |
| S0/a–Sab Galaxies             |                               |                                |
| $a_e$ vs. $h$                 | 0.76 ( $8.7 \times 10^{-5}$ ) | 0.57 (0.0081)                  |
| $L_{\text{bar}}$ vs. $h$      | 0.80 ( $2.7 \times 10^{-5}$ ) | 0.65 (0.0019)                  |
| $a_e$ vs. $R_{25}$            | 0.68 ( $9.2 \times 10^{-4}$ ) | 0.54 (0.013)                   |
| $L_{\text{bar}}$ vs. $R_{25}$ | 0.63 (0.0028)                 | 0.48 (0.032)                   |
| $a_e$ vs. $M_B$               | −0.58 (0.0077)                | −0.54 (0.014)                  |
| $L_{\text{bar}}$ vs. $M_B$    | −0.64 (0.0025)                | −0.58 (0.0079)                 |
| Sb Galaxies                   |                               |                                |
| $a_e$ vs. $h$                 | 0.67 (0.018)                  | 0.67 (0.017)                   |
| $L_{\text{bar}}$ vs. $h$      | 0.67 (0.018)                  | 0.76 (0.004)                   |
| $a_e$ vs. $R_{25}$            | 0.44 (0.15)                   | 0.27 (0.39)                    |
| $L_{\text{bar}}$ vs. $R_{25}$ | 0.43 (0.17)                   | 0.24 (0.46)                    |
| $a_e$ vs. $M_B$               | 0.01 (0.97)                   | 0.06 (0.85)                    |
| $L_{\text{bar}}$ vs. $M_B$    | 0.02 (0.95)                   | 0.06 (0.86)                    |

As for Table 3, but using only those galaxies with measured disc scale length  $h$  (see Section 3.3) and including correlations of bar size with  $h$ .

to be due, at least in part, to the fact that SB and SAB bars have distinctive sizes in late-type galaxies.

### 4.3 Bar Size and Bar Strength

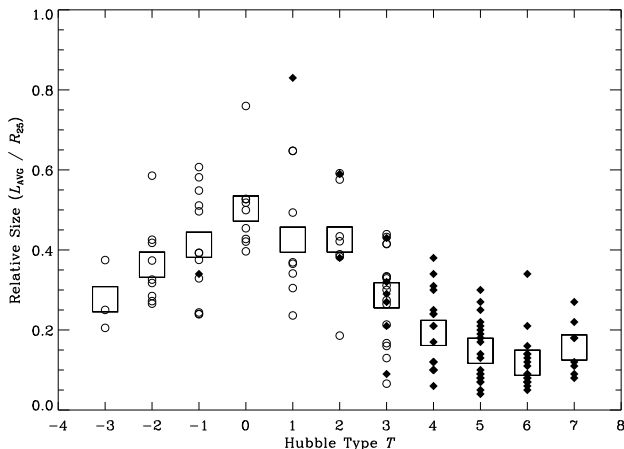
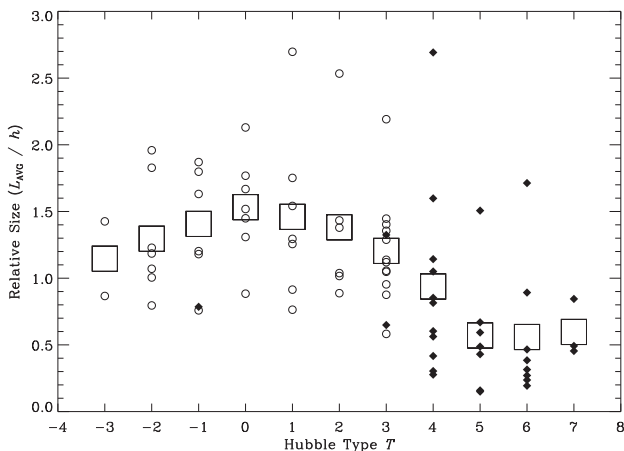
Strongly barred early-type galaxies (that is, S0–Sb galaxies with an RC3 bar classification of SB) typically have bar sizes roughly the same as those of early-type SAB galaxies (Table 2). The average SB bar is only  $\sim 10$ –35% larger than the average SAB bar for size in kpc or relative to  $R_{25}$ , and 2–3% *smaller* when size relative to disc scale length is used. K-S tests give probabilities of 11–94% (depending on how the size is measured) that the SB and SAB lengths come from the *same* parent distributions.

The parameter which *does* differ significantly between

**Table 5.** Mean Bar Size ( $L_{\text{avg}}$ ) for S0–Sd Galaxies

| Types      | $L_{\text{avg}}$ [kpc] | $L_{\text{avg}}/R_{25}$ | $L_{\text{avg}}/h$ |
|------------|------------------------|-------------------------|--------------------|
| All S0–Sab | $3.29 \pm 1.68$        | $0.37 \pm 0.13$         | $1.29 \pm 0.54$    |
| Sb         | $2.81 \pm 1.76$        | $0.28 \pm 0.11$         | $1.21 \pm 0.51$    |
| Sbc        | $2.35 \pm 1.22$        | $0.19 \pm 0.10$         | $0.92 \pm 0.70$    |
| Sc         | $1.60 \pm 0.96$        | $0.15 \pm 0.08$         | $0.57 \pm 0.46$    |
| Scd        | $1.15 \pm 0.55$        | $0.12 \pm 0.07$         | $0.56 \pm 0.52$    |
| Sd         | $1.30 \pm 0.50$        | $0.16 \pm 0.07$         | $0.58 \pm 0.23$    |
| All Sc–Sd  | $1.38 \pm 0.78$        | $0.14 \pm 0.07$         | $0.57 \pm 0.44$    |
| SB Sc–Sd   | $1.83 \pm 1.00$        | $0.19 \pm 0.07$         | $0.82 \pm 0.58$    |
| SAB Sc–Sd  | $1.14 \pm 0.50$        | $0.11 \pm 0.05$         | $0.40 \pm 0.22$    |

Relative and absolute sizes  $L_{\text{avg}}$  of bars for S0–Sd galaxies. The S0–Sab galaxies are from my sample, the Sbc–Sd galaxies are from Martin’s (1995) sample, and the Sb galaxies are from both. For my galaxies  $L_{\text{avg}}$  = the mean of  $a_e$  and  $L_{\text{bar}}$ , while  $L_{\text{avg}}$  = Martin’s measurements for galaxies from his sample.

**Figure 12.** As for Figure 11, but now showing size of bars relative to disc radius  $R_{25}$ .**Figure 13.** As for Figure 11, but now showing size of bars relative to the outer-disc exponential scale length  $h$ .

SB and SAB bars in early-type galaxies is, not surprisingly, the deprojected ellipticity ( $0.49 \pm 0.13$  for SB,  $0.36 \pm 0.15$  for SAB), with a K-S test giving only a 0.6% probability of the same parent distribution. Interestingly, this is *not* as true for the *observed* ellipticities: the mean ellipticity is still higher for SB galaxies ( $0.47 \pm 0.15$  versus  $0.39 \pm 0.14$  for SAB), but the K-S probability is now 22%.

Deprojected ellipticity does correlate with bar size for S0–Sb galaxies, but only weakly:  $r_s = 0.46$  and  $0.42$  ( $P = 1.2 \times 10^{-4}$  and  $4.5 \times 10^{-4}$ ) for  $a_e/R_{25}$  and  $a_e$  in kpc, respectively. These correlations are weaker when  $L_{\text{bar}}$  is used:  $r_s = 0.25$  and  $0.29$  ( $P = 0.041$  and  $0.021$ ) for  $L_{\text{bar}}/R_{25}$  and  $L_{\text{bar}}$  in kpc, respectively. (The correlations for bar size relative to disc scale length are weaker still:  $r_s = 0.09$  and  $P = 0.64$  for  $L_{\text{bar}}/h$ .) This generally agrees with Chapelon et al. (1999) and Laurikainen et al. (2002), who found very little correlation between deprojected ellipticity or bar axis ratio and bar size for their early-type spirals. It is also consistent with the correlation reported by Laine et al. (2002), who used  $a_e$  for bar sizes – especially since the latter authors’ samples included some Sc galaxies, for which the correlation is stronger (see below).

In late-type galaxies, SB bars are more elliptical than SAB bars (deprojected ellipticity  $0.64 \pm 0.18$  versus  $0.40 \pm 0.20$ ), just as for the early-type galaxies.<sup>7</sup> However, there is also a dramatic difference in bar size between late-type strong (SB) and weak (SAB) bars. On average, SB bars in Sc–Sd galaxies are almost *twice* the size of SAB bars (Table 5); a K-S test shows that this difference is significant at the 99.9% level for bar size relative to  $R_{25}$  (the significance is 99.2% for absolute sizes and 94% for sizes relative to  $h$ ). Since SB bars are also more elliptical than SAB bars, we should expect a strong correlation between bar size and deprojected ellipticity for the late-type bars, and this is indeed the case. For  $L_{\text{avg}}/R_{25}$  versus deprojected ellipticity,  $r_s = 0.73$  ( $P = 9.4 \times 10^{-9}$ ) for Sc–Sd bars, compared with only 0.36 ( $P = 0.0021$ ) for the S0–Sb bars. A similar result was found by Martinet & Friedli (1997) for a late-type (Sbc–Scd) subset of Martin’s galaxies and by Chapelon et al. (1999) for their “normal” (i.e., non-starbursting) Sbc and later-type galaxies.

There is some evidence for a stronger correlation between bar size and  $R_{25}$  (and perhaps also  $M_B$ ) when only late-type SB bars are considered: the Spearman correlation coefficient is 0.73 with a probability of  $P = 0.0013$  for  $L_{\text{avg}}$  versus  $R_{25}$ . In contrast, for SAB late-type galaxies  $r_s$  is only 0.29 with  $P = 0.21$ . A similar disparity exists for correlations between relative bar size and  $M_B$ , though they are not statistically significant for the main sample; when all of Martin’s Sc–Sd galaxies are included, the coefficients are  $-0.68$  ( $P = 4.5 \times 10^{-4}$ ) for SB bars versus  $-0.48$  ( $P = 0.0019$ ) for SAB bars.

Thus it appears that there may be a dichotomy between SB and SAB bars in the late-type galaxies, with SB bars perhaps retaining some of the characteristics (larger size, stronger correlation with  $R_{25}$  and  $M_B$ ) of both SB and SAB bars in early-type galaxies. It should be noted that there are about twice as many SAB as SB bars in the Sc–Sd galaxies

<sup>7</sup> This discussion omits the SBc galaxy NGC 2835, for which Martin (1995) lists a deprojected axis ratio of 1.0.

**Table 7.** Correlations Between Bar Size  $L_{\text{avg}}$  and Galaxy Properties – Galaxies from Martin (1995) Only

| Types                                     | $N$ | Pearson $r$                   | Spearman $r_s$ |
|---|-----|-------------------------------|----------------|
| Correlation with Disc Scale Length $h$    |     |                               |                |
| Sb  | 7   | 0.97 ( $2.1 \times 10^{-4}$ ) | 0.93 (0.0025)  |
| Sbc                                       | 16  | 0.65 (0.0064)                 | 0.48 (0.060)   |
| Sc-Sd                                     | 24  | -0.04 (0.87)                  | 0.02 (0.93)    |
| Correlation with Disc Size $R_{25}$       |     |                               |                |
| Sb  | 7   | 0.37 (0.41)                   | 0.79 (0.036)   |
| Sbc                                       | 16  | 0.77 ( $5.4 \times 10^{-4}$ ) | 0.69 (0.0032)  |
| Sc-Sd                                     | 24  | 0.09 (0.69)                   | 0.08 (0.71)    |
| Correlation with Absolute Magnitude $M_B$ |     |                               |                |
| Sb  | 7   | -0.19 (0.69)                  | -0.64 (0.12)   |
| Sbc                                       | 16  | -0.65 (0.0064)                | -0.68 (0.0038) |
| Sc-Sd                                     | 24  | -0.03 (0.89)                  | 0.00 (0.99)    |

As for Table 6, but using *all* galaxies from the Martin (1995) sample with plausible disc scale lengths from BBA98 (except for three Virgo cluster galaxies).

studied here; thus the overall weakness or absence of bar-size correlations for Sc-Sd galaxies is partly a combination of poor correlation for the SAB bars and the dichotomy in sizes between SB and SAB bars. However, even when Sc-Sd bars are analyzed independently in SB and SAB categories, there is still *no* correlation between bar size and exponential disc scale length.

## 5 DISCUSSION

### 5.1 Biases, Sample Incompleteness, and the Absolute Sizes of Bars

All the bars studied in this paper are in galaxies classified as barred (SB or SAB) in RC3. Because RC3 classifications are based on blue photographic plates, there is the possibility that some bars have been missed, for two reasons. First, as has been recognized for some time, bars can be hidden in optical images due to dust and star formation. This is probably not a large effect, *if* SAB galaxies are included in the “barred” category: Eskridge et al. (2000) found that the total (SB + SAB) bar fraction goes from  $65 \pm 3\%$  when using *B*-band images to  $73 \pm 3\%$  when using *H*-band images. However, they also found that a significant number of optically weak (SAB) galaxies (68%) become SB when classified in the IR, which suggests that many optically weak bars are really “disguised” strong bars.

The second potential bias is the possibility that *small* bars have been missed due to resolution (and possibly saturation) effects. Recent CCD and near-IR observations have uncovered large numbers of small, *inner* bars embedded inside large bars; most of these went unnoticed in earlier photographic surveys (see Erwin 2004). Some galaxies classed as unbarred turn out to have *nuclear* bars small enough to have been missed in low-resolution or nuclear-saturated photographic images (e.g., Buta 1991; Buta & Crocker 1991; Scorza et al. 1998). So the samples may be missing precisely those galaxies with the smallest bars.

An additional bias affects the absolute sizes (lengths in kpc). The samples studied here tend to exclude small, faint galaxies. The mean (and median) luminosity is  $M_B = -19.3$  for the S0 galaxies,  $-19.6$  for the S0/a-Sb galaxies in my sample, and  $-19.8$  for the Sb-Sd galaxies taken from Martin’s (1995) sample. This can be compared with the mean luminosities for cluster S0 galaxies ( $M_B = -18.9$ ) and spirals ( $M_B = -18.2$ ), from Jerjen & Tammann (1997): clearly, the bars studied here come from galaxies on the bright ends of the distributions. As we have seen, bar size generally scales with disc size and with galaxy luminosity; thus, smaller galaxies will have smaller bars. This means that the absolute-size distributions presented here (e.g., Figures 8 and 11) are biased towards larger bars, and the mean sizes are probably overestimates for the *complete* galaxy population.

### 5.2 Bar Sizes and Simulations

The only reasonable way to compare the sizes of real bars with those produced in *n*-body simulations is to use sizes relative to the disc scale length. In principle one can calculate sizes relative to  $R_{25}$  as well, but this requires estimating mass-to-light ratios and the star-formation history (e.g., Michel-Dansac & Wozniak 2004) and is thus prone to more uncertainties. In this section, I survey some recent *n*-body studies in an attempt to see how well or poorly they do at reproducing the relative sizes of real bars. I make no attempt to be comprehensive, and I am necessarily limited to those studies which provide both bar sizes and some indication of disc scale length in the region outside the bar (either as measured by the authors or via inspection of surface density profiles).

Table 8 summarizes results from eight different papers. In each case, I have included as many models from each study as possible, though in some cases additional models are left out because there were no bar or disc sizes for them. One thing is immediately apparent: *simulations tend to produce large bars*. Indeed, several simulations produce bars which are either at the upper end of the local distribution, or are larger than any seen in nearby galaxies. Except for two of the earlier simulations, no *n*-body bars are as small as typical Sc-Sd bars. (Ironically, one of these is the “early-type” model CS2 of Combes & Elmegreen 1993, which produced a shorter bar than their “late-type” model CSE.)

Holley-Bockelmann et al. (2005) argued that when bars are triggered by satellite interactions, rather than disc instabilities, “the length of the bar will depend on the mass and distance of the satellite. . . . The typical bar induced by this process will be much larger than those formed through internal disk instabilities.” Their final bar size of  $a_e/h \sim 2.6$  is indeed rather large: only two of the galaxies in my sample and one of Martin’s have bars that large (Figures 10 and 13). The  $a_e/h \sim 4$  bar which they report for their  $B_5$  simulation (no profiles shown) is clearly excessive. None the less, the fact that the bar size in their simulations depends on the details of the galaxy-satellite interaction is intriguing, because it suggests that bar sizes in real galaxies might provide clues to their host galaxies’ interaction/merger histories. The absence of real bars with  $a_e/h > 3$  could then indicate an upper limit on past bar-forming interactions.

**Table 6.** Correlations Between Bar Size  $L_{\text{avg}}$  and Galaxy Properties for S0–Sd Galaxies

| Types                                     | $N$ | Pearson $r$ ( $P$ )            | Spearman $r_s$ ( $P$ )         | $N$ | Pearson $r$ ( $P$ )           | Spearman $r_s$ ( $P$ )        |
|---|-----|--------------------------------|--------------------------------|-----|-------------------------------|-------------------------------|
| Correlation with Disc Size $R_{25}$       |     |                                |                                |     |                               |                               |
| All Galaxies                              |     |                                | Measured $h$ Only              |     |                               |                               |
| S0–Sab                                    | 48  | 0.76 ( $4.4 \times 10^{-10}$ ) | 0.75 ( $1.0 \times 10^{-9}$ )  | 24  | 0.72 ( $7.4 \times 10^{-5}$ ) | 0.66 ( $4.5 \times 10^{-4}$ ) |
| Sb–Sbc                                    | 40  | 0.58 ( $8.3 \times 10^{-5}$ )  | 0.49 (0.0013)                  | 19  | 0.45 (0.051)                  | 0.51 (0.025)                  |
| Sc–Sd                                     | 46  | 0.30 (0.043)                   | 0.31 (0.037)                   | 18  | 0.10 (0.68)                   | 0.12 (0.64)                   |
| Correlation with Disc Scale Length $h$    |     |                                |                                |     |                               |                               |
| All Galaxies                              |     |                                | Measured $h$ Only              |     |                               |                               |
| S0–Sab                                    |     |                                |                                | 24  | 0.70 ( $1.2 \times 10^{-4}$ ) | 0.61 ( $1.6 \times 10^{-3}$ ) |
| Sb–Sbc                                    |     |                                |                                | 19  | 0.32 (0.19)                   | 0.34 (0.15)                   |
| Sc–Sd                                     |     |                                |                                | 18  | 0.00 (1.00)                   | 0.05 (0.84)                   |
| Correlation with Absolute Magnitude $M_B$ |     |                                |                                |     |                               |                               |
| All Galaxies                              |     |                                | Measured $h$ Only              |     |                               |                               |
| S0–Sab                                    | 48  | −0.61 ( $3.7 \times 10^{-6}$ ) | −0.65 ( $6.4 \times 10^{-7}$ ) | 24  | −0.63 (0.0011)                | −0.62 (0.0013)                |
| Sb–Sbc                                    | 40  | −0.34 (0.033)                  | −0.34 (0.032)                  | 19  | −0.21 (0.39)                  | −0.40 (0.093)                 |
| Sc–Sd                                     | 46  | −0.24 (0.11)                   | −0.21 (0.16)                   | 18  | −0.06 (0.80)                  | −0.04 (0.89)                  |

For the S0–Sb galaxies from my sample,  $L_{\text{avg}}$  is the average of  $a_e$  and  $L_{\text{bar}}$ ; for Martin’s (1995) Sb–Sd galaxies, it is his visual measurement  $L_b(i)$ . For each correlation coefficient, the probability that the correlation is due to chance is given in parentheses. The Sb–Sbc correlations include galaxies from both my sample and from Martin (1995). “Measured  $h$  Only” means those galaxies with measured outer disc scale lengths.  $N$  is the number of galaxies in each subsample.

Taking this argument further, one could ask if the larger bars of early-type galaxies indicate a stronger role for interactions in their formation. In this vein, Noguchi (1996) argued that bars in early-type galaxies, with their “flat” major-axis profiles, are better produced by interactions than by spontaneous disc instabilities; the latter, he suggests, are responsible for late-type bars. When combined with the argument of Holley-Bockelmann et al., we seem to get a consistent picture: the differing characteristics of bars in early- and late-type galaxies indicate a greater role for interactions in the evolution of early-type galaxies. There is at least some observational evidence for this: Elmegreen et al. (1990) reported that, for early-type (Sa–Sb) galaxies, the SB fraction was higher in binary-galaxy systems than in groups or the field; for late-type galaxies, there was no trend with environment. This fits neatly into scenarios where evolution into or along the Hubble sequence is determined primarily by the number and strength of interactions and mergers; for example, recent simulations support the idea that the bulges and thick discs characteristic of early-type galaxies have grown through satellite accretion (e.g., Walker et al. 1996; Aguerri et al. 2001). Unfortunately, as Table 8 shows, both Berentzen et al. (1998) and Athanassoula & Misiriotis (2002) were able to produce extremely large bars via disc instabilities. Since flat bar profiles can also be produced this way (e.g., Sparke & Sellwood 1987; Combes & Elmegreen 1993; Athanassoula & Misiriotis 2002), it appears that satellite interaction may *not* be a unique explanation for early-type bars.

Athanassoula & Misiriotis (2002) and Athanassoula (2003) have emphasized the importance of angular momentum transfer in regulating the size of bars, based on their analysis of  $n$ -body simulations. Put simply, bar length is ultimately limited by the corotation radius; if a bar slows

down, the corotation radius moves further out in the disc and the bar can grow in length. A bar slows if it can lose angular momentum, primarily via resonances, to particles in the outer disc, the halo, and the bulge (if present). In principle, then, larger bars indicate galaxies where the bar was able to lose more angular momentum. This might explain the generally large bars of early-type galaxies, since these galaxies are more likely to have significant bulges which can act as angular momentum sinks for the bar. This might also explain why model B of Valenzuela & Klypin (2003) produces a relatively small bar, since in that model the halo – also an angular momentum sink – is less massive relative to the disc than in the A<sub>1</sub>/A<sub>2</sub> models. However, this still does not explain why *late*-type bars are as small as they are, since even the “bulge-less”  $n$ -body simulations (e.g., model MD of Athanassoula & Misiriotis 2002) produce bars at least a scale length in radius.

### 5.3 Some Implications for Secular Evolution

In the past decade, an increasingly popular idea has been that bars can drive long-term (“secular”) evolution of disc galaxies, perhaps even helping to determine the present-day Hubble sequence. The general argument is that bars, through gas inflow and vertical buckling, create or amplify bulges, thus shifting a galaxy from smaller to larger bulge/disc ratio (e.g., from being an Sc galaxy to being an Sb or Sa galaxy). In addition, it is suggested that the increasing central mass concentration produced by bar-driven gas inflow can end up turning the bar *into* a bulge. This is because a sufficiently strong central mass concentration can apparently *destroy* a bar, producing an axisymmetric, bulge-like remnant (Hasan & Norman 1990; Hasan et al. 1993; Norman et al. 1996; Berentzen et al. 1998).

**Table 8.** Relative Bar Sizes from  $n$ -Body Simulations

| Study                           | Model          | Type             | $R_{\text{bar}}$ | $h$  | $R_{\text{bar}}/h$ | Notes |
|---------------------------------|----------------|------------------|------------------|------|--------------------|-------|
| Pfenniger & Friedli (1991)      |                | $n$ -body        | 10               | 17   | 0.6                |       |
| Combes & Elmegreen (1993)       | CS2            | $n$ -body        | 6                | 9.4  | 0.6                | 1     |
|                                 | CSE            | $n$ -body        | 9.5              | 5.2  | 1.8                | 2     |
| Friedli & Benz (1993)           | A              | $n$ -body+gas    | 6                | 7    | 0.9                | 3     |
| Berentzen et al. (1998)         | A              | $n$ -body        | 8                | 2.2  | 3.6                | 4     |
|                                 | B              | $n$ -body+gas    | 7                | 2.9  | 2.4                | 5     |
| Athanasoula & Misiriotis (2002) | MDB            | $n$ -body        | 3.1–3.5          | 1.1  | 2.8–3.2            | 6     |
|                                 | MD             | $n$ -body        | 2.1–3.2          | 1.4  | 1.5–2.3            | 6     |
| Valenzuela & Klypin (2003)      | A <sub>1</sub> | $n$ -body        | 6.2–6.7          | 4.5  | 1.4–1.5            | 7     |
|                                 | A <sub>2</sub> | $n$ -body        | 4.5–5.5          | 4.2  | 1.1–1.3            | 7     |
|                                 | B              | $n$ -body        | 4.2–5.0          | 5.0  | 0.8–1.0            | 7     |
| Holley-Bockelmann et al. (2005) | F <sub>5</sub> | $n$ -body        | 0.026            | 0.01 | 2.6                | 8     |
| Immeli et al. (2004)            | F              | $n$ -body+gas+SF | 3–4.5            | 1.9  | 1.6–2.1            | 9     |

“Model” refers to a given model from the study in question; “Type” indicates the type of simulation (“SF” = star formation);  $R_{\text{bar}}$  and  $h$  are the bar semimajor axis and disc scale length in model units (usually kpc).

Notes: (1) “Early-type” model galaxy. (2) “Late-type” model galaxy. (3) Bar size measured at  $t = 1000$  from their Fig. 2, disc scale length for  $r > 10$  kpc from their Fig. 3a. (4) Values at  $t = 65$ . (5) Values at  $t = 20$ –65. (6) Range in bar sizes is their  $L_{b/a}$ – $L_{\text{phase}}$ , which corresponds to my  $a_e$ – $L_{\text{bar}}$ ; sizes are averages of values in their Table 1 (to match time of profiles shown in their Fig. 5);  $h$  for the MDB model is from Lia Athanasoula (private communication). (7) Range in bar sizes using their two measurement techniques. (8) Bar size underestimates full bar length (their Fig. 3), so probably matches  $a_e$  better than  $L_{\text{bar}}$ . (9) Range in bar sizes for  $t = 2.8$ –3.8 Gyr (their Fig. 14).

A recent elaboration on the scenario of secular evolution via bar dissolution, with specific predictions for bar *sizes*, is that of Bournaud & Combes (2002). They posit multiple rounds of a sequence where bars form, weaken or are destroyed via mass inflow, and then reform due to gas accretion by the disc (see also Sellwood & Moore 1999). In their simulations, later (i.e., second, third, or even fourth!) bars are progressively *shorter* than earlier bars. The implication is that early-type spirals (and S0’s), whose larger bulges are built out of multiple rounds of bar formation and bar-driven inflow, should have smaller bars. Unfortunately, this is clearly incompatible with the Hubble sequence as we see it today.<sup>8</sup>

However, secular changes in bar size may still be relevant if we drop the idea of bar destruction. Most of the  $n$ -body bars mentioned in the previous section have sizes measured near the end of the simulation, and can thus be considered “mature” bars. But in almost all  $n$ -body simulations, bars lose angular momentum, slow down, and increase in length as time goes by: older bars are longer than younger bars. The growth is usually fairly mild, but can sometimes be dramatic – for example, Valenzuela & Klypin (2003) mention that the bar in their A<sub>2</sub> simulation *triples* in absolute length (from 1.5 to 4.5–5 kpc) between  $t = 3$  and 6 Gyr. Since the disc scale length varies by  $\lesssim 20\%$ , the *relative* size of the bar also triples, from  $\sim 0.4h$  to  $\sim 1.2h$ . This neatly spans the range in typical relative sizes between Sc–Sd galaxies and Sa–Sb galaxies (Table 5 and Figure 13).

Could the difference in bar sizes between early- and late-type galaxies, or the scatter in sizes for a given region of the Hubble sequence, be at least partly a matter of bar *age*? This might also explain the lack of a correlation between bar size and other galaxy properties, especially disc scale length, for the late-type galaxies (Section 4.2), if disc scale length primarily affects or determines the *final* size of a bar. Bars in Sc–Sd galaxies would then be young and/or still growing rapidly, and thus less likely to show correlations with disc size.

This idea – younger, shorter, and fast-growing bars in Sc–Sd galaxies, older and longer bars in early-type galaxies – is also consistent with the simulations and arguments of Friedli & Benz (1995) and Martin & Friedli (1997). They combined  $n$ -body simulations with gas and star formation, and noted that “young” bars ( $< 500$  Myr old in their simulations) had star formation concentrated along the bar major axis, something observed in at least some SBc galaxies, while older bars tended to have star formation confined to the nucleus, the ends of the bars, and an inner ring/spiral surrounding the bar, a pattern more often seen in early-type galaxies. Based on this, they suggested that barred Sc galaxies could evolve into barred Sb galaxies. (The fact that subsequent star formation is generally restricted to the ends of the bar and an inner ring might also indicate that star formation helps transform late-type “exponential” bars into early-type “flat” bars, by preferentially adding stars near the ends of the bar.) It would be interesting to see if there is a correlation between star-formation patterns and bar sizes in, e.g., Sbc–Sd galaxies: are smaller bars in fact more likely to have “young” star-formation patterns? There is actually a hint of this in the sample of Martin & Friedli (1997): they classified eleven bars into three categories (A, B, C) based on the distribution of H II regions, and then associated these

<sup>8</sup> At least some of the difference may be due to the particular mode of accretion used by Bournaud & Combes (2002), such that alternate accretion scenarios might produce more realistic distributions of bar sizes (Frédéric Bournaud, private communication.)

categories with increasing age, based on their simulations. The mean relative bar sizes of the three groups are, in order of increasing age,  $L_{avg}/R_{25} = 0.19, 0.28$ , and  $0.32$ , which does agree with the scenario; but the sample is really too small for this to be a valid test.

A problem with this idea is the fact that, in the few simulations where gas has been included and bar length at different times is reported (e.g., Berentzen et al. 1998; Immeli et al. 2004), the bar does *not* grow significantly; it may even *shrink* slightly. This may be because the bar gains angular momentum from the gas inflow it drives, thus keeping its pattern speed constant or increasing and keeping corotation at a small radius. This would seem to mean that bars in Sc–Sd galaxies, which generally have abundant gas, should not grow significantly; this might even help explain why their bars are generally small! It may be that once enough of the gas within corotation has been exhausted (e.g., converted to stars), the bars *can* grow; but whether this is possible, and whether the bars can grow large enough, awaits further simulation. (Both of the studies mentioned above produced bars larger than those of typical *early*-type galaxies, so it isn't clear how relevant they are to late-type bars.)

The alternative to these scenarios of secular evolution is that there is something fundamentally different between early- and late-type disc galaxies, which is reflected in their different bar properties. It would be fruitful to examine more carefully why some simulations produce larger bars than others (see, for example, the discussions in Athanassoula 2003; Valenzuela & Klypin 2003), and whether there are any parameters (e.g., relative halo mass, halo structure and kinematics, and in particular gas content) which can reliably produce the small bars of late-type galaxies.

On a separate note, it is interesting to compare the field and Virgo S0 galaxies in my sample. A popular scenario for creating *cluster* S0 galaxies is ram-pressure stripping of spirals which fall into a cluster and encounter its intracluster medium at high speed (e.g., Quilis et al. 2000). If removal of a spiral galaxy's gas – and subsequent aging of its stellar population without new star formation – is *all* that happens, then we might expect other properties, such as bar size, to remain unchanged. Since the most numerous bright spiral types are Sbc and Sc (e.g., Eskridge et al. 2002), we should on average see smaller bars in cluster S0's – *if* conversion of infalling spirals is the primary formation mechanism. However, as I showed in Section 4.1, Virgo Cluster S0's tend if anything to have *larger* bars than field S0's, and their bars are certainly consistent with the general field S0–Sb population. This suggests that cluster S0's are probably not just stripped and aged spirals, or else that they are preferentially formed from *early-type* spirals. Quilis et al. note that other mechanisms may be needed to produce larger bulges and thicker discs in stripped spirals in order to make the end products more like S0 galaxies; such mechanisms must also, it seems, ensure that cluster S0's end up with large bars.

#### 5.4 Finding Bars at High Redshift

Although the samples analyzed here do not extend to very faint magnitudes, there is no evidence for any trend in *relative* bar size with magnitude or  $R_{25}$  (Figure 14). This suggests that smaller and fainter galaxies should follow the gen-

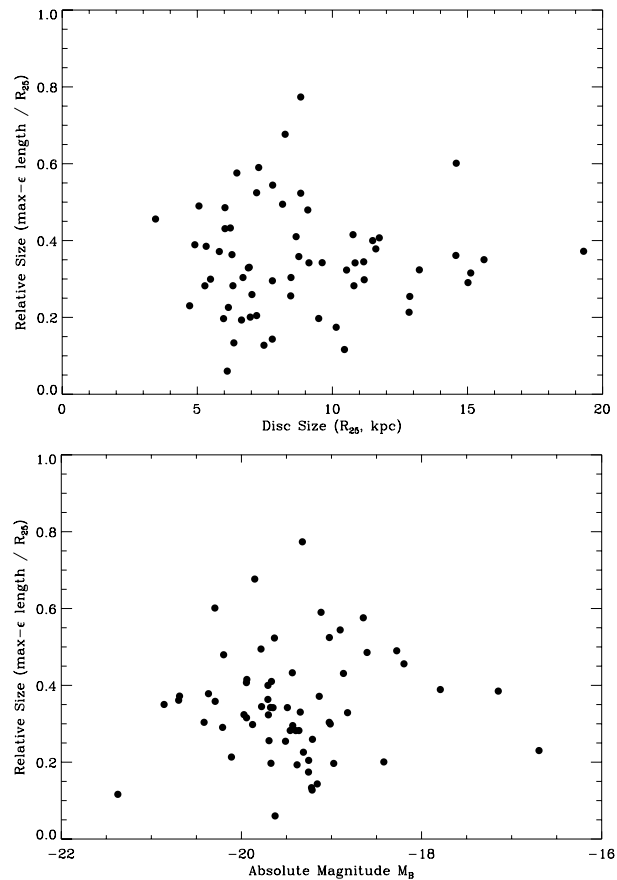


**Figure 14.** Relative bar size  $a_{\epsilon}/R_{25}$  versus disc size (top) and galaxy luminosity (bottom) for S0–Sb galaxies. Relative bar size shows no correlation with either galaxy size or luminosity; this suggests that galaxies smaller and/or less luminous than the sample probably have a similar range of relative bar sizes.

eral bar-size–luminosity and bar-size–disc-size correlations found here, at least for Hubble types earlier than Sc. So if high- $z$  galaxy samples include significant numbers of faint galaxies, they will probably include bars which are small in absolute (kpc) terms, and thus difficult to detect.

The important point is that – in the absence of any evolutionary effects – the absolute size of bars, and thus their detectability, depends on the size, luminosity, and Hubble types of the galaxies being studied. Thus, a proper measure of bar fractions as a function of redshift requires careful sample selection: the low-redshift and high-redshift samples must contain galaxies with a similar distribution of disc sizes or absolute magnitudes. The latter is probably easier to achieve, but evolutionary corrections will almost certainly need to be applied. Disc isophotal size will probably also evolve with redshift, in ways perhaps less easy to model. (Recall the subtle bias introduced by an isophotal size limit in my sample, leading to an Sb subsample with smaller scale lengths and absolute bar sizes than the S0–Sab bars; see Section 4.1.) The best sample-matching might therefore be in terms of disc scale lengths — assuming, of course, that *they* do not evolve significantly.

Recently, van den Bergh et al. (2002) analyzed the detectability of bars and spiral structure with redshift by artificially redshifting and resampling  $B$ -band images from the

Ohio State University Bright Spiral Galaxy Survey (BSGS; Eskridge et al. 2002) to match  $z = 0.7$  Hubble Deep Field (HDF) exposures. They argued that most of the strong bars in the BSGS galaxies would still be detectable at  $z = 0.7$ ; the apparent absence of such bars in real HDF galaxies at  $z \sim 0.7$  (e.g., van den Bergh et al. 2000) is then, they suggest, a genuine effect. But lurking behind this is the assumption that the BSGS is a reasonable match to high- $z$  HDF galaxies. As their Figure 2 shows, the BSGS does live up to its name: the magnitude distribution peaks at  $M_B \approx -20.2$ , and essentially all of the galaxies are brighter than the *mean* magnitude ( $-18.2$ ) of local spirals found by Jerjen & Tammann (1997). Van den Bergh et al. noted that deep *HST* images, such as the HDF, will sample significantly fainter galaxies, even in the absence of luminosity evolution. This means that – assuming no *bar* evolution – the average bar in the HDF sample will probably be smaller (in kpc) than the average BSGS bar, and therefore harder to detect (see the discussion of bar-size detectability versus redshift in Sheth et al. 2003).

In striking contrast to the apparent absence of optical bars at high  $z$  in the HDF, Sheth et al. (2003) found at least four barred galaxies with  $z \sim 1$  in the HDF by using NICMOS images, which suggests that bandshifting effects are important. More recent studies based on higher-resolution ACS imaging (Elmegreen et al. 2004; Jogee et al. 2004) find comparable fractions of bars at low and high  $z$ ; this is eloquent confirmation of the parallel importance of resolution, as Sheth et al. also emphasized.

Sheth et al. reported an average bar semimajor axis of 6 kpc for their high- $z$ , NICMOS-detected bars, and argued that this was unusually large when compared with local galaxies – specifically, when compared with the BIMA Survey of Nearby Galaxies (SONG) sample.<sup>9</sup> But are the bars they found really so large? The BIMA SONG galaxies are dominated by intermediate and late types (21 of its 29 barred galaxies are Sbc or later), and thus should include mostly smaller bars. In Figure 15 I plot the semimajor axes of their high- $z$  bars in the context of the entire Hubble sequence. The high- $z$  bar sizes are based on my inspection of their NICMOS ellipse fits, with  $L_{\text{avg}}$  = the average of  $a_e$  and  $a_{10}$ . In general, I find smaller values of  $a_e$  than they do (2.4–6.5 kpc, versus their 4–8 kpc), probably because they use the absolute peak in ellipticity, which can be due to spiral arms outside the bar itself. Because these bar sizes are *observed* (i.e., no deprojection was attempted), I compare them with the observed sizes of local bars. Figure 15 shows that the high- $z$  bars Sheth et al. found are unusually large only in the context of late-type spirals; they are large but plausible for early-type spirals.

The mean  $L_{\text{avg}}$  of the high- $z$  bars is 4.7 kpc, very close to the NICMOS3 detection limit Sheth et al. suggest for  $z \sim 1$ . One might then ask, following Sheth et al., whether finding the number of bars of that size (e.g., two with  $L_{\text{avg}} > 4.7$  kpc) in high- $z$  spirals is at all meaningful in the context of local galaxies. In Figure 15, there are 6 out of 113 local barred spirals with projected  $L_{\text{avg}} > 4.7$  kpc. This translates to 6 out of  $\sim 160$  local spirals of *all* bar classes – assuming

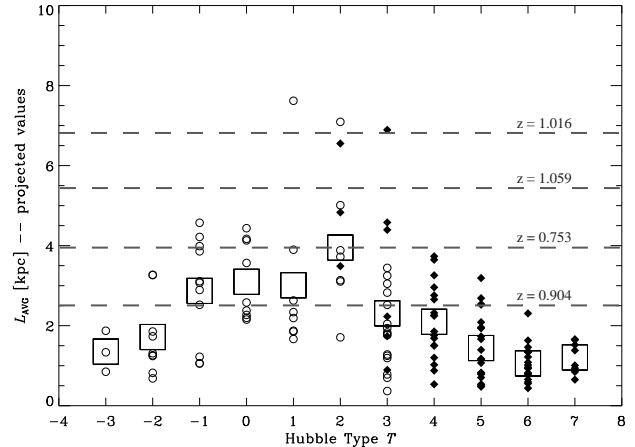


**Figure 15.** As for Figure 11, but now showing *observed* (i.e., not deprojected) bar sizes. Sizes for the four high- $z$  bars of Sheth et al. (2003) are indicated by dashed lines.

that  $\sim 70\%$  of local spirals with  $D_{25} \geq 2.0'$  and  $a/b \leq 2.0$  have RC3 classifications of SB or SAB (Erwin 2005) – for a local frequency of  $\approx 4 \pm 2\%$ . Sheth et al. found their four barred galaxies in a sample of 95 disclike galaxies with  $z > 0.7$ ; they noted that the total number would drop to 31 (and three barred galaxies) if the magnitude cutoff of Abraham et al. (1999) was used. Regardless of how the parent sample is defined, the frequency of large bars at high- $z$  ( $2/95 = 2 \pm 1\%$  or  $2/31 = 6 \pm 4\%$ ) appears consistent with the local frequency. Of course, this analysis assumes the parent samples are comparable, which is probably not true. For example, the faintest of their high- $z$  barred galaxies has  $H \approx 26$ , which they suggest corresponds to rest-frame  $M_B \approx -16$ . This is fainter than any of the galaxies in my sample, Martin’s (1995) sample, *or* the BIMA SONG sample.

Finally, I note that the much larger (though currently incomplete) sample of  $z = 0.7$ – $1.0$  disc galaxies studied by Jogee et al. (2004) seems to have typical bar semimajor axes  $\sim 3$  kpc, very close to the average S0–Sb bar sizes in my sample (Table 2). Again, this suggests that bar sizes at  $z \sim 1$  were similar to bar sizes in the local universe, and that high- $z$  studies will naturally select against the small bars characteristic of late-type spirals.

## 6 SUMMARY

I have presented a study of bar sizes in disc galaxies, using a sample of 65 nearby S0–Sb galaxies as well as the published bar sizes for 70 nearby Sb–Sd galaxies from Martin (1995). The main results are summarized below.

(i) Bars in early-type (S0–Sb) galaxies have mean absolute sizes (semimajor axis) of  $\sim 3.3$  kpc, and mean relative sizes of  $\sim 0.38 R_{25}$  and  $\sim 1.4 h$  (where  $h$  is the exponential disc scale length).

(ii) For these galaxies, the sizes of bars *relative to disc scale length* is roughly constant with Hubble type. The Sb galaxies in my sample appear to have smaller bars relative to  $R_{25}$  in comparison to the S0–Sab galaxies because the Sb galaxies have, on average, *larger* values of  $R_{25}/h$ . A diameter-limited selection criterion then leads to smaller

<sup>9</sup> Note that they discuss all sizes, and plot their ellipse fits, in terms of *diameters*.

average scale lengths for these galaxies and thus bars with smaller average absolute sizes ( $\sim 2.5$  kpc) as well.

(iii) As has been noted earlier, bars in early-type (S0–Sb) galaxies are larger than those in late-type (Sc–Sd) galaxies. This is true regardless of how bar size is measured; bar size relative to disc scale length appears to be the most robust measurement, and the least vulnerable to selection effects. On average, early-type bars are  $\sim 2.5$  times larger than late-type bars, which have mean sizes of  $\sim 1.5$  kpc,  $0.14 R_{25}$ , and  $0.6 h$ . Sbc galaxies have bars intermediate in size between the early and late types.

(iv) Early-type bars show strong correlations of bar size with  $R_{25}$  and  $h$ ; these correlations are stronger than the known correlation of bar size with  $M_B$ . But late-type bars as a whole show only weak correlations of bar size with  $R_{25}$  and  $M_B$ , and *no* correlation with  $h$  at all.

(v) Strong (SB) and weak (SAB) bars in early-type galaxies differ primarily in ellipticity; they are very similar in size. But late-type galaxies exhibit a real dichotomy: SB bars in Sc–Sd galaxies are on average twice the size of SAB bars, and the SB bars have stronger correlations of bar size with  $R_{25}$  and  $M_B$ .

(vi) Comparison with a number of recent  $n$ -body studies suggests that simulations usually produce relatively large bars (bar size  $\gtrsim 1.5h$ ), including some bars larger than those seen in real galaxies. The small bars typical of late-type galaxies (bar size  $\sim 0.6h$ ) are rare in simulations.

(vii) Comparison with local bars shows that the recently discovered  $z \sim 1$  bars of Sheth et al. (2003) have sizes typical of those in *early*-type (S0–Sb) galaxies. Because bar size scales with disc size (and, less strongly, with  $M_B$ ) for all but the latest Hubble types, and because smaller bars are harder to detect at high redshift, attempts to compare bar frequencies at different redshifts must be careful to use similar samples of galaxies – ideally samples with similar disc scale lengths.

## ACKNOWLEDGMENTS

I am grateful to Paul Schechter for observations made at the MDM Telescope, to Hans Deeg for observations made at the Isaac Newton Telescope, and especially to Juan Carlos Vega Beltrán for his help in obtaining observations at Nordic Optical Telescope; I also thank Johan Knapen for a  $K$ -band image of NGC 4725. I enjoyed helpful and interesting conversations with a number of people, including Andrew Cardwell, Ignacio Trujillo, Alister Graham, Alfonso López Aguerri, Michael Pohlen, John Beckman, Victor Debattista, and Octavio Valenzuela. Kartik Sheth, Karin Menendez-Delmestre, Witold Maciejewski, and Lia Athanassoula provided insightful comments on early drafts, and Seppo Laine was quite helpful at clarifying some of the complexities of deprojecting ellipses. Finally, I thank the referee, Eija Laurikainen, for a careful reading and several suggestions that improved the paper.

This research is (partially) based on data from the ING Archive, and on observations made with both the Isaac Newton Group of Telescopes, operated on behalf of the UK Particle Physics and Astronomy Research Council (PPARC) and the Nederlandse Organisatie voor Wetenschappelijk Onderzoek (NWO) on the island of La Palma, and the Nordic Op-

tical Telescope, operated on the island of La Palma jointly by Denmark, Finland, Iceland, Norway, and Sweden. Both the ING and NOT are part of the Spanish Observatorio del Roque de los Muchachos of the Instituto de Astrofísica de Canarias. I also used images from the Barred and Ringed Spirals (BARS) database, for which time was awarded by the Comité Científico Internacional of the Canary Islands Observatories.

This research made use of the NASA/IPAC Extragalactic Database (NED) which is operated by the Jet Propulsion Laboratory, California Institute of Technology, under contract with the National Aeronautics and Space Administration. It also made use of the Lyon-Meudon Extragalactic Database (LEDa; part of HyperLeda at <http://leda.univ-lyon1.fr/>).

## REFERENCES

- Abraham R. G., Merrifield M. R., Ellis R. S., Tanvir N. R., & Brinchmann J., 1999, MNRAS, 308, 569
- Aguerrí J. A. L., Muñoz-Tuñón C., Varela A. M., & Prieto M., 2000, A&A, 361, 841
- Aguerrí J. A. L., Balcells M., & Peletier R. F., 2001, A&A, 367, 428
- Aguerrí J. A. L., Debattista V. P., & Corsini E. M., MNRAS, 338, 465
- Athanassoula E., 2003, MNRAS, 341, 1179
- Athanassoula E., 2004, in Dark Matter in Galaxies, IAU Symposium 220, ed. S. D. Ryder, D. J. Pisano, M. A. Walker, & K. C. Freeman (San Francisco: Astronomical Society of the Pacific), 255
- Athanassoula E., Misiriotis A., 2002, MNRAS, 330, 35
- Baggett W. E., Baggett S. M., Anderson K. S. J., 1998, AJ, 116, 1626 (BBA98)
- Berentzen I., Heller C. H., Shlosman I., & Fricke K. J., 1998, MNRAS, 300, 49
- Binney J., Merrifield M., 1998, Galactic Astronomy. Princeton Univ. Press, Princeton, NJ
- Bosma A., Ekers R. D., Lequeux J., 1977, A&A, 57, 97
- Bournaud F., Combes F., 2002, A&A, 392, 83
- Buta R., 1986, ApJS, 61, 609
- Buta R., 1991, ApJ, 370, 130
- Buta R., 1995, ApJS, 96, 39
- Buta R., Crocker D. A., 1991, AJ, 102, 1715
- Buta R., Block D. L., 2001, ApJ, 550, 243
- Chapelon S., Contini T., Davoust E., 1999, A&A, 345, 81
- Combes F., Elmegreen B. G., 1993, A&A, 271, 391
- Courteau S., 1996, ApJS, 103, 363
- Debattista V. P., Sellwood J. A., 2000, ApJ, 543, 704
- de Jong R. S., 1996, A&AS, 118, 557
- de Jong R. S., van der Kruit P. C., 1994, A&AS, 106, 451
- de Vaucouleurs G., de Vaucouleurs A., Corwin H. G., Buta R. J., Paturel G., Fouqué P., 1991, Third Reference Catalogue of Bright Galaxies. Springer-Verlag, New York (RC3)
- Elmegreen B. G., Elmegreen D. M., 1985, ApJ, 288, 438 (EE85)
- Elmegreen D. M., Elmegreen B. G., Bellin A. D. 1990, ApJ, 364, 415
- Elmegreen B. G., Elmegreen D. M., Hirst A. C. 2004, ApJ, 612, 191

- Erwin P., 2004, *A&A*, 415, 941
- Erwin P., 2005, in prep
- Erwin P., Sparke L. S., 1999, *ApJ*, 512, L37
- Erwin P., Sparke L. S., 2002, *AJ*, 124, 65
- Erwin P., Sparke L. S., 2003, *ApJS*, 146, 299
- Erwin P., Vega Beltrán J. C., Graham A. W., Beckman J. E., 2003, *ApJ*, 597, 929
- Erwin P., Beckman J. E., Pohlen M., 2005, *ApJL*, 626, L81
- Eskridge P. B. et al., 2000, *AJ*, 119, 536
- Eskridge P. B. et al., 2002, *ApJS*, 143, 73
- Freedman W. et al., 2001, *ApJ*, 553, 47
- Freeman K. C., 1970, *ApJ*, 160, 811
- Frei Z., Guhathakurta P., Gunn J. E., Tyson J. A., 1996, *AJ*, 111, 174
- Friedli D., Benz W., 1993, *A&A*, 268, 65
- Friedli D., Benz W., 1995, *A&A*, 301, 649
- Gavazzi G., Boselli A., 1996, *ApL&C*, 35, 1
- Graham A. W., 2001, *AJ*, 121, 820
- Greusard D., Friedli D., Wozniak H., Martinet L., Martin P., 2000, *A&AS*, 145, 425
- Grosbøl P. J., 1985, *A&AS*, 60, 261
- Hasan H., & Norman C. 1990, *ApJ*, 361, 69
- Hasan H., Pfenniger D., & Norman C., 1993, *ApJ*, 409, 91
- Holley-Bockelmann K., Weinberg M. D., Katz N., 2005, *MNRAS*, submitted (astro-ph/0306374)
- Immeli A., Samland M., Gerhard O., Westera P., 2004, *A&A*, 413, 547
- Jerjen H., Tammann G. A., 1997, *A&A*, 321, 713
- Jogee S. et al., 2004, *ApJL*, 615, L105
- Jungwiert B., Combes F., Axon D. J., 1997, *A&AS*, 125, 479
- Kenney J. D. P., Carlstrom J. E., Young J. S. 1993, *ApJ*, 418, 687
- Kenney J. D. P., Rubin V. C., Planesas P., Young J. S. 1995, *ApJ*, 438, 135
- Koopmann R. A., Kenney J. D. P., 1998, *ApJ*, 497, L75
- Kormendy J., 1977, *ApJ*, 214, 359
- Kormendy J., 1979, *ApJ*, 227, 714
- Kormendy J., 1982, in *Morphology and Dynamics of Galaxies: Twelfth Advanced Course of the Swiss Society of Astronomy and Astrophysics*, ed. L. Martinet & M. Mayor (Sauverny: Observatoire de Genève), 113
- Kornreich D. A., Haynes M. P., & Lovelace R. V. E., 1998, *AJ*, 116, 2154
- Kornreich D. A., Haynes M. P., Lovelace R. V. E., & van Zee L., 2000, *AJ*, 120, 139
- Krumm N., & Shane W. W., 1982, *A&A*, 116, 237
- Laine S., Shlosman I., Knapen J. H., Peletier R. F., 2002, *ApJ*, 567, 97
- Laurikainen E., Salo H. 2002, *MNRAS*, 337, 1118
- Laurikainen E., Salo H., Rautiainen P. 2002, *MNRAS*, 331, 880
- Laurikainen E., Salo H., Buta R., Vasylyev S., 2004, *MNRAS*, 355, 125
- Lourenso S., Beckman J. E., 2001, *Ap&SS*, 276, 1161
- Martin P., 1995, *AJ*, 109, 2428
- Martin P., Friedli D., 1997, *A&A*, 326, 449
- Martinet L., Friedli D., 1997, *A&A*, 323, 363
- Michel-Dansac L., Wozniak H., 2004, *A&A*, 421, 863
- Möllenhoff C., Heidt J., 2001, *A&A*, 368, 16
- Nilson P., 1973, *Uppsala General Catalog of Galaxies*, Uppsala Astron. Obs. Annals, 5, 1
- Noguchi M., 1996, *ApJ*, 469, 605
- Norman C., Sellwood J. A., & Hasan H. 1996, *ApJ*, 462, 114
- Ohta K., Hamabe M., Wakamatsu K.-I., 1990, *ApJ*, 357, 71
- Pedlar A., Howley P., Axon D. J., Unger S. W., 1992, *MNRAS*, 259, 369
- Pfenniger D., Friedli D., 1991, *A&A*, 252, 75
- Press W. H., Teukolsky S. A., Vetterling W. T., Flannery B. P., 1996, *Numerical Recipes* (Cambridge: Cambridge U. Press)
- Quilis V., Moore B., Bower R., 2000, *Science*, 288, 1617
- Quillen A. C., Frogel J. A., Gonzalez R. A., 1994, *ApJ*, 437, 162
- Regan M. W., Elmegreen D. M., 1997, *AJ*, 114, 965
- Saha A., Sandage A., Labhardt L., Schwengler H., Tammann G. A., Panagia N., Macchetto F. D. 1995, *ApJ*, 438, 8
- Sakamoto K., Okumura S. K., Ishizuki S., Scoville N. Z., 1999, *ApJ*, 124, 403
- Sánchez-Portal M., Díaz A. I., Terlevich R., Terlevich E., Álvarez Álvarez M., & Aretxaga I., 2000, *MNRAS*, 312, 2124, 403
- Seigar M. S., & James P. A., 1998, *MNRAS*, 299, 672
- Schneider S. E., 1989, *ApJ*, 343, 94
- Scorza C., Bender R., Winkelman C., Capaccioli M., & Macchetto D. F., 1998, *A&AS*, 131, 265
- Sellwood J. A., 2003, *ApJ*, 587, 638
- Sellwood J. A., Moore E. M., 1999, *ApJ*, 510, 125
- Sheth K., Regan M. W., Scoville N. Z., Strubbe L. E., 2003, *ApJ*, 592, L13
- Shlosman I., Peletier R. F., Knapen J. H. 2000, *ApJ*, 535, L83
- Sil'chenko O. K., Moiseev A. V., Afanasiev V. L., Chavushyan V. H., Valdes, J. R., 2003, *ApJ*, 591, 185
- Sparke L. S., Sellwood J. A., 1987, *MNRAS*, 225, 653
- Tonry J. L., Dressler A., Blakeslee J. P., Ajhar E. A., Fletcher A. B., Luppino G. A., Metzger M. R., Moore C. B., 2001, *ApJ*, 546, 681
- Tully R. B., Verheijen M. A. W., Pierce M. J., Huang J.-S., Wainscoat R. J., 1996, *AJ*, 112, 2471
- Valenzuela O., Klypin A., 2003, *MNRAS*, 345, 406
- van den Bergh S., 1976, *ApJ*, 206, 883
- van den Bergh S., Cohen J. G., Hogg D. W., Blandford R. 2000, *AJ*, 120, 2190
- van den Bergh S., Abraham R. G., Whyte L. F., Merrifield M. R., Eskridge P. B., Frogel J. A., Pogge R., 2002, *AJ*, 123, 2913
- Walker I. R., Mihos J. C., Hernquist L., 1996, *ApJ*, 460, 121
- Weinberg M. D., Katz N., 2002, *ApJ*, 580, 627
- Wozniak H., Pierce, M. J., 1991, *A&AS*, 88, 325
- Wozniak H., Friedli D., Martinet L., Martin P., Bratschi P., 1995, *A&AS*, 111, 115

## APPENDIX A: NOTES ON INDIVIDUAL GALAXIES

Unless otherwise noted, all disc scale lengths were measured using the azimuthally averaged profile outside the bar region. If no clear, exponential profile could be determined,

then no fit was performed. Specific exceptions, and cases where the non-exponentiality can be traced to specific morphological features (or observational problems), are listed below. Galaxies which met the sample selection criteria but which are not included in the final set of measurements are indicated by names enclosed by brackets, or else listed at the end of each subsample.

### A1 The WIYN Sample (Field S0–Sa)

For most of these galaxies, the relevant details (including sources for the distance measurements) are discussed in Erwin & Sparke (2003). Here, I provide additional notes, primarily on measurements of outer disc scale lengths.

**NGC 936:** Type II outer-disc profile.

**NGC 2859:** Strong outer ring produces extreme Type II profile.

**NGC 2880:** Outer profile is non-exponential, flattening at large radii (probably dominated by bulge light). The inclination is based on the region of maximum ellipticity, where the disc appears to dominate ( $r \approx 50''$ ), but no clear slope can be determined.

**NGC 2962:** Type II outer-disc profile.

**NGC 3412:** Type II outer-disc profile.

**NGC 3489:** Bar measurements are from an unpublished WHT-INGRID  $H$ -band image, due to strong dust extinction in the optical.

**NGC 3729:** The outer-disc scale length and revised outer-disc orientation are from a Sloan  $r$ -band image obtained with the INT-WFC (Erwin, Pohlen, & Beckman 2005, in prep), since the WIYN images were taken during full moon.

**NGC 3945:** Strong outer ring produces extreme Type II profile; the inclination has been updated using a high-quality  $r$ -band image from the Wide Field Camera of the 2.5m Isaac Newton Telescope (INT-WFC, La Palma; Erwin, Pohlen, & Beckman 2005, in prep).

**NGC 4143:** The outer-disc scale length is from a Sloan  $r$ -band image obtained with the INT-WFC (Erwin, Pohlen, & Beckman 2005, in prep).

**NGC 4203:** Type II outer-disc profile. The length  $L_{\text{bar}}$  of the bar, based on the ellipticity minimum, is undoubtedly an overestimate; since this galaxy is nearly face-on and lacks spiral arms, the ellipse-fit measurements  $a_{\text{min}}$  and  $a_{10}$  are misleading or undefined.

**NGC 4245:** Outer disc orientation and scale-length measurements are from a Sloan  $r$ -band image obtained with the INT-WFC (Erwin, Pohlen, & Beckman 2005, in prep).

**NGC 4665:** Type II outer-disc profile.

The following galaxies in the WIYN Sample were eliminated because they appeared to lack bars, or because they were too dusty and highly inclined for accurate measurements of their bars (for details, see Erwin & Sparke 2003): NGC 2655, 2685, 3032, and 4310.

### A2 Virgo S0

**NGC 4267:** All measurements are from Nordic Optical Telescope (NOT)  $R$ -band images; bar measurements agree very well with the  $H$ -band measurements of Jungwiert et al. (1997).

**NGC 4340:** All measurements are from MDM  $R$ -band images (bar measurements agree very well with  $J$ - and  $K$ -band measurements from BARS Project images), except for the outer-disc scale length, which is from the  $R$ -band image of Frei et al. (1996).

**NGC 4371:** Bar measurements are from WIYN  $R$ -band images measurements, but the outer-disc inclination and scale length are from deeper INT-WFC  $r$ -band images (Erwin, Pohlen, & Beckman 2005, in prep).

**[NGC 4435]:** Since this galaxy is apparently interacting with its neighbor NGC 4438, and possibly edge-on as well (e.g., Kenney et al. 1995), I excluded it from the sample.

**NGC 4477:** All measurements are from the  $R$ -band image of Frei et al. (1996).

**[NGC 4531]:** This galaxy has a dusty inner spiral, but no evidence for a bar, despite its SB0 classification.

**NGC 4596:** All measurements are from BARS Project  $R$ -band images (taken with the Prime Focus Camera of the Isaac Newton Telescope), except for the outer-disc orientation and inclination, which are from a deeper  $I$ -band image.

**NGC 4608:** All measurements are from NOT  $R$ -band images.

**NGC 4612:** All measurements are from MDM  $R$ -band images; these agree well with measurements made using the  $R$ -band image of Frei et al. (1996).

**NGC 4754:** All measurements from WIYN  $R$ -band images, except that the outer-disc scale length was determined from the  $R$ -band image of Frei et al. (1996), due to strong background variations in the WIYN image.

### A3 Field Sab–Sb

Unless otherwise noted, bar and disc measurements for these galaxies were made using  $R$ -band images from the Nordic Optical Telescope (NOT), supplemented in some cases by  $J$  and  $K_s$  images from the William Herschel Telescope (WHT).

**[NGC 278]:** Both optical and near-IR images indicate that this SAB galaxy is not actually barred (e.g., Eskridge et al. 2000).

**[NGC 2146]:** This galaxy is severely distorted and almost certainly interacting; near-IR images suggest there is probably no bar.

**NGC 2712:** Bar measurements are from near-IR images, due to strong dust extinction in the  $R$ -band. The outer-disc scale length is from an archival  $R$ -band INT-WFC image; disc orientation is from H I kinematics (Krumm & Shane 1982).

**NGC 3351:** Bar measurements are from the  $r$ -band image of Frei et al. (1996); the outer-disc profile is Type II. Distance is from *HST* Cepheid measurements (Freedman et al. 2001).

**NGC 3368:** Because the (outer) bar is very dusty in the optical, measurements were made using the  $K$ -band image of Möllenhoff & Heidt (2001). The outer-disc PA and inclination are from WIYN  $R$ -band images, which agree well with measurements made using the Frei et al. (1996)  $R$ -band image and with kinematic line-of-nodes from both the H I study of Schneider (1989), as quoted in Sakamoto et al. (1999), and the near-nuclear 2D spectroscopy of Sil'chenko et al. (2003). Type II outer-disc profile.

**[NGC 3455]:** Inspection of  $R$ -band and NICMOS2

F160W images strongly suggests that this SAB galaxy is not actually barred.

**NGC 3504:** Bar measurements are from a BARS Project *I*-band image from the NOT (no *R*-band images are available). Outer disc orientation is from Grosbøl (1985) and Kenney et al. (1993). Although the inclination is uncertain, deprojection is not a major issue given that the bar is almost aligned with the outer-disc major axis.

**NGC 3982:** Type II outer-disc profile. Bar measurements are from a NICMOS2 F160W image; outer-disc PA is from Sánchez-Portal et al. (2000).

**NGC 4102:** Type II outer-disc profile. Bar measurements are from a NICMOS3 F160W image.

**NGC 4151:** Bar measurements and outer-disc scale length are from a BARS Project *R*-band image (taken with the INT Prime Focus Camera). Outer disc orientation and inclination from the H I kinematics (Bosma et al. 1977; Pedlar et al. 1992).

**NGC 4319:** Bar measurements are from archival Jacob Kapteyn Telescope *R*-band images, obtained from the Isaac Newton Group Archive, and from an unpublished WHT *J*-band image. Outer disc orientation and inclination is from Grosbøl (1985).

**NGC 4725:** The large-scale bar in this galaxy is peculiar and somewhat difficult to measure, since it twists sharply with radius (it is similar to NGC 3185 and NGC 5377 in this respect). None the less, there is a clear ellipticity maximum very close to the inner ring (which itself defines  $L_{\text{bar}}$ ); this agrees fairly well with the measurements of Martin (1995) and Chapelon et al. (1999). Although the galaxy is somewhat dusty, the *R*-band bar measurements agree very well with measurements made with a *K*-band image kindly provided by Johan Knapen. The outer disc scale length is from the *r*-band image of Frei et al. (1996); distance is from *HST* Cepheid measurements (Freedman et al. 2001). The ellipticity of the outer disc is uncertain, due to the presence of two strong spiral arms, so the inclination is based in inverting the Tully-Fisher relation using the *H*-band magnitude of Gavazzi & Boselli (1996), the H I width  $W_{20}$  from RC3, the Cepheid distance, and the *H*-band Tully-Fisher relation as given in Binney & Merrifield (1998, p. 425).

[**NGC 4941:** Greusard et al. (2000) argued that this galaxy has a nuclear bar but no large-scale bar, based on their near-IR images; on the other hand, Eskridge et al. (2002) classified it as SAB using lower-resolution *H*-band images, so it is not clear whether this is a single- or double-barred galaxy.

**NGC 5740:** Bar measurements are from near-IR images, due to strong dust extinction in the *R*-band. The outer-disc scale length, from fits to  $r < 100''$  (this is another Type III profile, so the disc beyond that radius has a shallower slope) agrees beautifully with Courteau’s (1996) *r*-band  $h = 18.3''$ .

**NGC 5806:** The bar presence is uncertain, at least in the *R*-band, though there is a clear ellipticity peak. The outer surface-brightness profile is Type III; the disc scale length is from the extended exponential region ( $r \approx 55$ – $100''$ ) outside the bar. This scale length matches the *r*-band scale length ( $28.8''$ ) of Courteau (1996) quite well, though not the *V*-band major-axis scale length ( $15''$ ) of Baggett et al. (1998).

**NGC 5832:**  $a_e$  is taken from a minimum in the PA.

**NGC 5957:**  $a_e$  is taken from a maximum in the PA.

**NGC 6012:** There are several ellipticity maxima in the ellipse fits within the bar; in this case,  $a_e$  is taken from the extremal value of the position angle. The outer disc orientation is from the *R*-band image; since the outer ellipticity is uncertain, the inclination is based on inverting the Tully-Fisher relation, using the *H*-band magnitude of de Jong & van der Kruit (1994), the H I width  $W_{20}$  from RC3, the LEDA distance, and the *H*-band Tully-Fisher relation as given in (Binney & Merrifield 1998, p. 425). The outer-disc scale length was measured from an INT-WFC *r*-band image (Erwin, Pohlen, & Beckman 2005, in prep).

**NGC 7177:** Bar and disc measurements are from an archival INT-WFC *R*-band image. The outer-disc scale length is from the  $r = 35$ – $60''$  region, and agrees very well with measurements by de Jong & van der Kruit (1994) and Graham (2001). Outside this region, the profile flattens; this is another Type III profile.

**UGC 3685:** The outer-disc scale length was measured from an INT-WFC *r*-band image (Erwin, Pohlen, & Beckman 2005, in prep). The outer-disc inclination is from Kornreich et al. (1998), with PA from H I kinematics Kornreich et al. (2000).

#### A4 Data for Galaxies from Martin (1995)

For the galaxies of Martin (1995), I took total blue magnitudes ( $B_{tc}$ ) from LEDA. Distances are mostly from LEDA as well, using the velocities corrected for Virgo-centric motion and  $H_0 = 75 \text{ km s}^{-1} \text{ Mpc}^{-1}$ , except for cases where more accurate distances were available. These were mainly *HST* Cepheid distances from Freedman et al. (2001), which I used for NGC 925, 1365, 3198, and 5457. In two cases, I used distances to galaxies in the same group as one of Martin’s galaxies: NGC 4236 is in the same group as NGC 2403 (M81), which has an *HST* Cepheid distance, while NGC 5236 is in the same group as NGC 5253 ( $D = 4.2 \text{ Mpc}$  from Cepheids; Saha et al. 1995) and NGC 5128 ( $D = 4.2 \text{ Mpc}$  from surface-brightness fluctuations; Tonry et al. 2001).

Some of the galaxies in Table 1 of Martin (1995) have incorrect numerical Hubble types ( $T$ ) listed, though the full RC3 types are correct: NGC 1156, 1288, 1433, 3614, 4214, 4304, 5350, and IC 1953. Finally, “NGC 4891” is really NGC 4397, and “New1” is MCG-01-03-085 (also listed as “Shapley-Ames 1” in NED).